

## Fuzzy-reasoning-based robust vibration controller for drivetrain mechanism with various control input updating timings

Heisei Yonezawa<sup>a</sup>, Ansei Yonezawa<sup>b</sup>, Takashi Hatano<sup>c</sup>, Shigeki Hiramatsu<sup>c</sup>, Chiaki Nishidome<sup>d</sup>, Itsuro Kajiwara<sup>a,\*</sup>

<sup>a</sup> Division of Mechanical and Aerospace Engineering, Hokkaido University, N13 , W8, Kita-ku, Sapporo 060-8628, Japan

<sup>b</sup> Division of Human Mechanical Systems and Design, Hokkaido University, N13 , W8, Kita-ku, Sapporo 060-8628, Japan

<sup>c</sup> Mazda Motor Corporation, 3-1 Shinchi, Fuchu-cho, Aki-gun, Hiroshima 730-8670, Japan

<sup>d</sup> CATEC Inc., Ono-building 3F, 4-24-7, Taito, Taito-ku, Tokyo 110-0016, Japan



### ARTICLE INFO

**Keywords:**

Powertrain  
Transient oscillations  
Active damping  
Control cycle limitation  
Fuzzy logic  
Sampled-data control

### ABSTRACT

For active vibration control of powertrain oscillations, the purpose of this research is to present a simple fuzzy-reasoning-based compensation strategy for a time-varying control cycle limitation of an actuator. A simplified drivetrain dynamics model is shown, and the simulation configuration with the control cycle limitation is constructed. A model predictive compensation using a sampled-data controller is employed to tackle the maximal phase delay of the control input due to the time-varying control cycle. The control input update timing, which is perturbed from that of the fixed periodical controller, is expressed as fuzzy sets such as "Approximately past step" and "Approximately future step". Based on these fuzzy sets, the Tsukamoto-type fuzzy reasoning with only four intuitive rules can flexibly infer unknown control inputs updated at various timings. Simulation verifications demonstrate that the 2-norm of the vibration performance by the proposed method is reduced by more than 27.8% compared to other previous controllers. Moreover, it is revealed that the better transient performance can be maintained even with 10% plant parameter variations, indicating the high robustness of the proposed damping controller.

### 1. Introduction

The driving condition with an abrupt torque change (tip-in/tip-out) and the nonlinear characteristic of gear backlash excite transient vibrations of a vehicle powertrain, making the comfortability and drivability considerably poor [1]. To suppress these vibrations without increasing the vehicle's weight, active vibration control utilizing an existing actuator must be introduced [2].

Active damping controllers for powertrains have been reported in many previous papers. In one previous study [2], a Linear-Quadratic-Gaussian (LQG) controller with an observer was designed based on the performance index to guarantee the dynamic performance and the fuel economy. To compensate for nonlinearity and flexibility of a powertrain, a mode-switching-based active control algorithm composed of the sliding mode technique and PID control was proposed [3]. The  $H_\infty$  synthesis problem was established for a drivetrain servo mechanism, and the robustness was experimentally tested [4]. However, in these previous studies [2–4], the limitations originating from actuator dynamics such as delays of realization of the control input are not addressed. Focusing on torque delivery dynamics during crossing in backlash, a model-based torque shaping controller was developed by introducing a soft

\* Corresponding author.

E-mail address: [ikajiwara@eng.hokudai.ac.jp](mailto:ikajiwara@eng.hokudai.ac.jp) (I. Kajiwara).

## Nomenclature

$M_B$	mass of the vehicle body in a simplified drivetrain [kg]
$m_G$	mass of the intermediate part in a simplified drivetrain [kg]
$M_E$	mass of the actuator in a simplified drivetrain [kg]
$K_C$	spring connected with $M_B$ [N/m]
$K_D$	spring between $M_B$ and $m_G$ [N/m]
$K_G$	spring between $M_E$ and $m_G$ [N/m]
$C_C$	damper connected with $M_B$ [Ns/m]
$C_D$	damper between $M_B$ and $m_G$ [Ns/m]
$C_G$	damper between $M_E$ and $m_G$ [Ns/m]
$C_{cl}$	damper of $M_E$ [Ns/m]
$A_p$	state matrix of the state equation of the plant
$B_{p1}$	disturbance matrix of the state equation of the plant
$B_{p2}$	input matrix of the state equation of the plant
$C_p$	output matrix of the state equation of the plant
$D_{p1}$	direct transmission matrix for $w_p$ of the state equation of the plant
$D_{p2}$	direct transmission matrix for $u$ of the state equation of the plant
$x_p$	state vector of the plant
$u$	control input [N]
$w_p$	disturbance including force due to backlash [N]
$y_p$	measured output (Vehicle body vibration $X_B$ )
$X_B$	vibration response of $M_B$ [m]
$x_G$	vibration response of $m_G$ [m]
$X_E$	vibration response of $M_E$ [m]
$\delta$	dead zone width
$Sw$	switching parameter to express the dead-zone effect due to backlash
$OKG$	constant term of spring force in the backlash model
$\Delta T_{cont}$	fixed control period of a sampled-data controller [s]
$k$	the number of calculation steps of a sampled-data controller
$u(k)$	control command value from a sampled-data controller at $k\Delta T_{cont}$
$A_{pd}$	coefficient matrix of the discrete-time state equation of the plant
$B_{p1d}$	coefficient matrix of the discrete-time state equation of the plant
$B_{p2d}$	coefficient matrix of the discrete-time state equation of the plant
$C_{pd}$	coefficient matrix of the discrete-time state equation of the plant
$D_{p1d}$	coefficient matrix of the discrete-time state equation of the plant
$D_{p2d}$	coefficient matrix of the discrete-time state equation of the plant
$x_{pd}$	state vector of the discretized plant
$i$	the number of steps of a real-time simulation in the model predictive processing
$N_{pre}$	the total number of steps of a real-time simulation
$\Delta T_{predict}$	calculation interval of a real-time simulation [s]
$r$	target signal of the vehicle body response to be realized [m]
$A_c$	coefficient matrix of the state-space representation of a sampled-data controller
$B_c$	coefficient matrix of the state-space representation of a sampled-data controller
$C_c$	coefficient matrix of the state-space representation of a sampled-data controller
$D_c$	coefficient matrix of the state-space representation of a sampled-data controller
$x_c$	state vector of the sampled-data controller
$z_1$	controlled variable in a generalized plant with respect to $X_B$
$z_2$	controlled variable in a generalized plant with respect to $u$
$s$	variable in Laplace transform
$P(s)$	plant model used in a generalized plant for sampled-data controller design
$W_y(s)$	frequency weighting function with respect to the vehicle body vibration
$\tilde{W}_y(s)$	transfer function including $\epsilon_1$ as a part of $W_y(s)$
$M(s)$	transfer function including $\epsilon_2$ as a part of $W_y(s)$
$W_u(s)$	frequency weighting function with respect to the control input
$\epsilon_1$	design parameter of $\tilde{W}_y(s)$ [Hz]
$\epsilon_2$	design parameter of $M(s)$ [Hz]
$t$	time within $k\Delta T_{cont} < t < (k+1)\Delta T_{cont}$ [s]

$t^*$	time defined as $t^* = t - k\Delta T_{cont}$ within $0 < t^* < \Delta T_{cont}$ [s]
$h_{future}^t$	membership function of fuzzy set “about future ( $\Delta T_{cont}$ )”
$h_{past}^t$	membership function of fuzzy set “about past (0)”
$h_{middle}^t$	membership function of fuzzy set “about middle ( $1/2\Delta T_{cont}$ )”
$h_{Big}^{cy}$	membership function of fuzzy set “Big”
$h_{small}^{cy}$	membership function of fuzzy set “Small”
$ \dot{y}_p _{max}$	the maximal value in the input space of $h_{Big}^{cy}$ and $h_{small}^{cy}$
$w_1$	degree of match of fuzzy rule (Rule 1)
$w_2$	degree of match of fuzzy rule (Rule 2)
$w_3$	degree of match of fuzzy rule (Rule 3)
$w_4$	degree of match of fuzzy rule (Rule 4)
$h_{future}^u$	membership function of fuzzy set “About $u(k + 1)$ ”
$h_{past}^u$	membership function of fuzzy set “About $u(k)$ ”
$\Delta u$	difference between the control command values at the past and future steps
$u_1$	crisp output inferred from fuzzy rule (Rule 1)
$u_2$	crisp output inferred from fuzzy rule (Rule 2)
$u_3$	crisp output inferred from fuzzy rule (Rule 3)
$u_4$	crisp output inferred from fuzzy rule (Rule 4)
$u_{Fuzzy}$	resultant inference output from the Tsukamoto-type inference system [N]

landing reference governor approach [5]. A notable point of this controller is reduction in clunk due to backlash via the simple configuration. Nevertheless, the effects of actuator dynamics on the damping performance are not dealt with [5].

Among the previous works, model predictive control (MPC) becomes most popular choice in the various forms. For undesired oscillations due to an abrupt torque change and backlash, the effectiveness of MPC, which was implemented online as receding horizon optimal control with a quadratic form, was experimentally investigated [6]. The feature of this work is use of a high-fidelity drivetrain model developed to capture the detailed mechanism [6]. In [7,8], switching control strategies composed of multiple predictive controllers successfully cope with the nonlinearity in a powertrain. In the engine control structure [9], the MPC controller can provide ideal responses including no error states such as excessive jerks and transient vibrations. However, the traditional MPC involves heavy computational burdens to solve the optimization problem online. In addition, as implied by [6,9], the traditional MPC is deeply dependent on accurate models. Therefore, difficulties in modeling of more complicated powertrains with the control cycle limitation described later hinder the control systems from being both simple and robust. In [10], a horizon-1 MPC scheme based on flexible Lyapunov functions was compared with traditional PID controllers, demonstrating that the MPC can handle both the drivetrain damping and physical constraints. However, this work does not consider the time-varying control cycle limitation described below.

An engine, which is a power resource for powertrains, has been also utilized as an effective actuator for active damping thanks to its cost, market penetration rates, and high power. With strict environmental regulations, investigations on novel-form engines based on clean energy (i.e., alternative fuels) such as hydrogen engines and biomass fuels have been attractive topics [11]. This trend will boost the importance of active damping techniques that consider mechanical limitations originating from dynamic characteristics of an engine.

However, due to the mechanical processes shown in Fig. 1, an engine cannot freely update the generated control input values at a fixed time interval which is synchronized with that of a digital controller. The control input can only be updated at the moment when a crankshaft rotates by a predetermined angle, resulting in the following control cycle limitations.

- (a) Compared with the natural frequency (1–10 Hz) to be controlled, the control cycles (i.e., actual updating intervals of control inputs) are significantly extended. This leads to increase in the discretization errors with implementation of a digital vibration controller.
- (b) Depending on engine speed, variation of the timings at which the control input can be updated occurs. That is, the actuator has time-varying control cycles.

Many studies on dynamics and vibration controls of powertrains including an engine as well as HVs equipped with it as power sources have been conducted [12–14]. Modeling of an engine with a fixed maximal delay enables systematic design of the  $H_\infty$  vibration controller [15]. Nevertheless, this controller does not compensate for the time-varying characteristic (b). Real-time predictive controllers were proposed to cope with the engine delay [16,17]. These approaches are based on the idea of Smith predictor including control-oriented drivetrain models, and the excellent transient responses were confirmed via actual test vehicles. Even though an engine is used as the active damping actuator [16,17], the above control cycle limitations are not sufficiently addressed. A gear shift control strategy was constructed based on linear quadratic regulator (LQR) and Extended Kalman filter (EKF) [18]. In [18], detailed dynamics of realization of the engine torque are considered. However, this study does not focus on simplicity of the control strategy.

Since an engine as the actuator is restricted by its slow dynamics, it was proposed that additional actuators are combined with an engine [19]. In [19], the friction brake was also utilized as the active damping actuator, resulting in extension to multi-input drivetrain

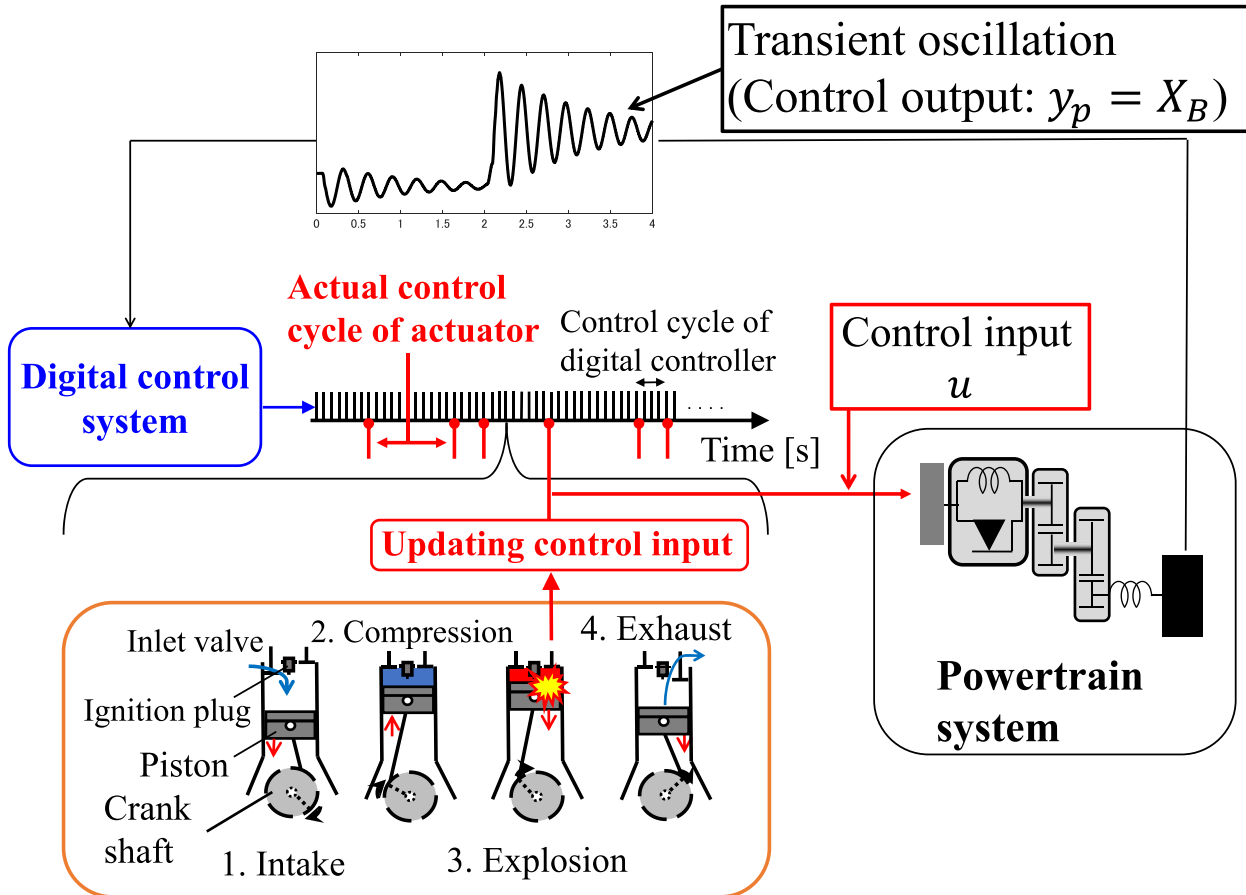


**Fig. 1.** Control cycle limitation due to the mechanical process to update control input.

**Table 1**

Literature review of control systems applied to drivetrain dynamics.

Approach	Refs.	Details and contributions	Room for improvement compared to this study
LQG	(2017) [2]	• A Linear-Quadratic-Gaussian (LQG) controller to guarantee the dynamic performance.	• Not addressing the limitations originating from actuator dynamics.
PD controller with backlash handling	(2021) [5]	• A soft-landing reference governor approach for reduction in clunk due to backlash.	• Not addressing the effects of actuator dynamics on the damping performance.
MPC	(2018) [6] (2018) [9] (2016) [10]	• A MPC with a high-fidelity driveline model for backlash compensation. • A MPC algorithm to generate an ideal response without excessive jerks and vibrations. • A MPC scheme based on flexible Lyapunov functions.	• Heavy computational burdens for optimization. • Difficulty in accurate modeling of complicated powertrains. • Not addressing the control cycle constraints.
$H_\infty$ synthesis	(2003) [15]	• A systematic design process of $H_\infty$ vibration controller.	• Not addressing the control cycle constraints.
Predictive control	(2008) [17]	• Real-time predictive controller based on the idea of Smith predictor.	• Not sufficiently addressing the control cycle constraints, especially for (a).
Gear shifting controller	(2021) [18]	• A gear shift control strategy based on LQR and EKF.	• Not focusing on simplicity of control systems.
Additional actuators	(2016) [19]	• A friction brake combined with an engine for active damping.	• Complicated control system architecture. • Not addressing the time-varying control cycle.
Disturbance rejection control	(2020) [20]	• A PD controller with an adaptive disturbance observer for addressing the time-varying characteristic of an engine.	• Not addressing the discretization error issue (a) by digital vibration controller implementation. • Difficulty in realizing sufficient vibration reduction and robustness. • No previous works that apply fuzzy logic to the control cycle constraints.
Fuzzy logic	(2022) [24] (2015) [26] (2018) [27]	• A dual-closed loop fuzzy PI controller to reduce vehicle jerk. • A fuzzy logic torque controller for active drivetrain damping. • A fuzzy logic switching strategy between LQR and a linear quadratic tracking (LQT) controller to ensure both drivability and comfortability.	• A lot of fuzzy rules and membership functions, leading to complicated structures.
Sampled-data controller	(2021) [21]	• A model predictive compensation using the sampled-data $H_2$ controller for addressing the control period problems (a) and (b).	• Not sufficiently addressing the time-varying control cycle. • No verifications of robustness. • Difficulty in ensuring robust vibration reduction.

vibration systems. However, addition of another actuator other than an engine makes the control system architectures more complicated. Moreover, no compensations for the time-varying control cycle (b) are presented [19].

Recently, a remarkable work on the active damping of internal combustion engine powered powertrains was reported [20]. The reported disturbance rejection approach can explicitly address the time-varying characteristic of an engine. The active damping system is composed of a PD controller and an adaptive disturbance observer (ADO) that is applied to a real-time estimation of harmonic disturbances. However, this approach does not consider the discretization error issue (a) that is due to the digital vibration controller implementation. Moreover, employing a conventional PD controller as the base damping strategy makes it difficult to obtain the sufficient vibration reduction and the robustness.

Consequently, all of the above previous works do not address both the control cycle limitation problems (a) and (b) simultaneously. Furthermore, to the best of our knowledge, there are no studies that realize a simple and intuitive (i.e., human-thought-like) control strategy with ease of understanding the compensation mechanism. Difficulties in accurate modeling of complicated powertrains, which include the time-varying control cycle as well as plant parameter's uncertainty, become barriers against realizing both simplicity and robustness of the control system.

Recently, our previous work [21] presented an active vibration control system to deal with both the problems (a) and (b) due to the control cycle limitation. This is based on the model predictive compensation using the servo-type sampled-data  $H_2$  controller for successfully addressing the discretization errors and the phase delay of control input induced by the time-varying control cycle. Nevertheless, this previous controller compensates for only the maximal phase delay of control inputs, and dealing with various control input update timings of the actuator is insufficient. Hence, there is a possibility that the previous approach alone fails to ensure the robustness of vibration suppression performances against plant variations.

Based on the previous work [21], this research explicitly tackles the variation of timings at which the control input is updated by the actuator. To provide both simplicity and robustness for the active damping system, fuzzy logic is effectively introduced.

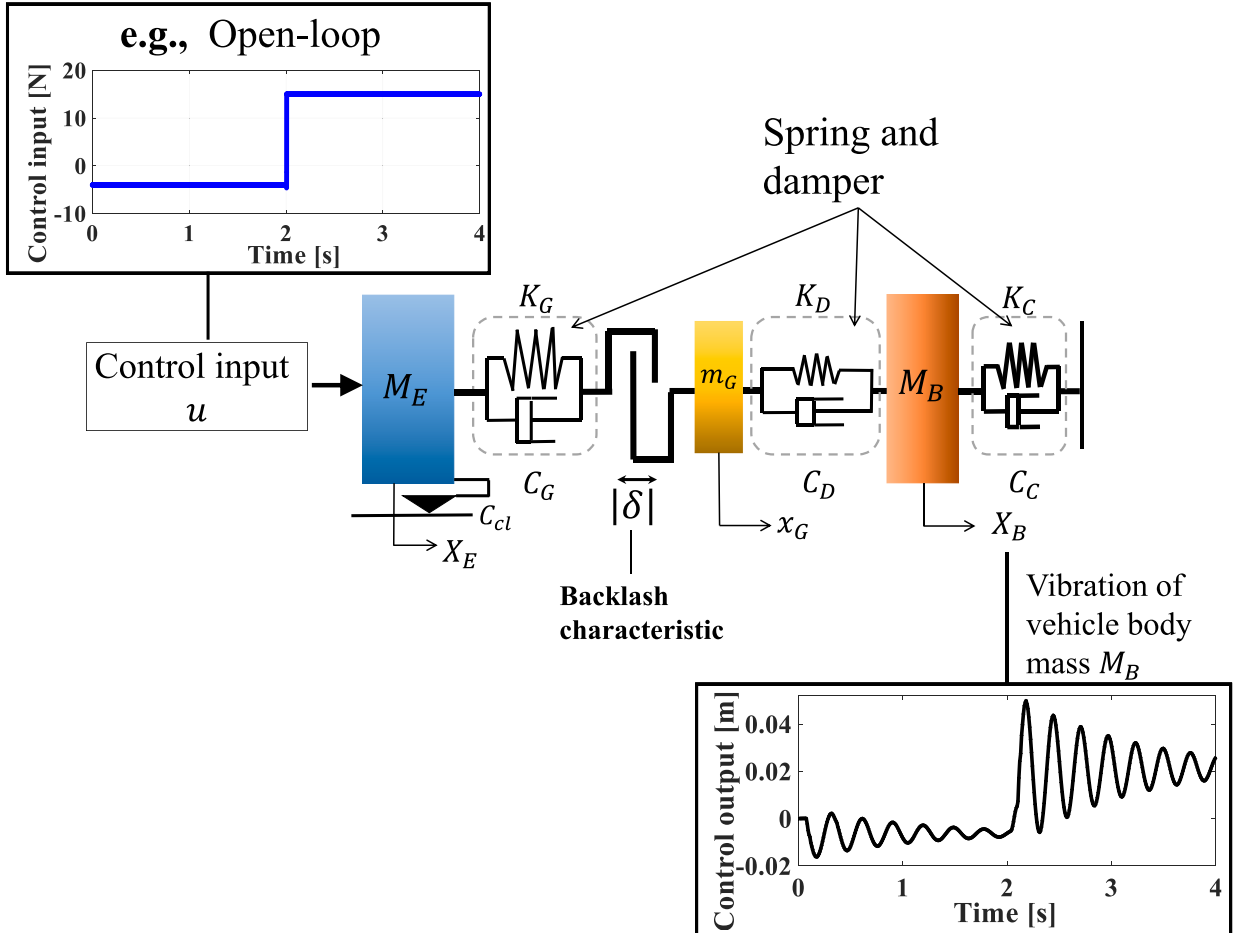


Fig. 2. Simplified drivetrain dynamics model.

Fuzzy theory is a powerful mathematical tool, which enables successfully dealing with uncertain and complicated mechanical systems based on linguistic and ambiguous variables [22,23]. Since its fundamental idea was first proposed by L.A. Zadeh, many researchers have applied fuzzy theory to a wide range of applications in control engineering [22,23]. One of the remarkable features of fuzzy logic is the robustness against situations where accurate system information cannot be obtained due to fragmentary modeling as well as plant parameter variations. For dynamics and vibration controls of powertrains, the successful application examples have been exhibited [24,25]. A fuzzy logic torque controller consisting of 7 fuzzy sets for two input variables and 13 fuzzy sets for an output variable was presented to attenuate drivetrain oscillations of a 4WD EV [26]. To ensure both drivability and comfortability in a sudden torque change situation, a fuzzy logic switching strategy between a LQR and a linear quadratic tracking (LQT) controller was proposed [27]. One group proposed a novel fuzzy logic gear shifting controller that is combined with an optimization algorithm such as the Interactive Adaptive-Weight Genetic Algorithm for an internal combustion engine vehicle [28].

However, there are no previous works that apply fuzzy logic to the control cycle limitation of an actuator in active drivetrain oscillation damping. In addition, because the fuzzy logic controllers applied to the above previous powertrain controls tend to have a large number of the inference rules, they lead to difficulty in handling and burden on implementation for designers. For example, above 40 fuzzy rules need to be set for the application of a fuzzy PI controller [24].

Compared to this paper, the literature reviews regarding the existing similar works mentioned above are also summarized in Table 1. Table 1 indicates the lacks in each similar work in the rightmost column "Room for improvement compared to this study". The main contributions and novelty of this paper are to fulfill these literature gaps.

This research proposes a simple fuzzy-reasoning-based compensation that imitates intuitive human-thought-like decisions for variations in the updating timings of the control input. The control input updating timing, which is perturbed from that of the fixed periodical damping controller, is expressed as fuzzy sets such as "Approximately past step" and "Approximately future step". Based on the Tsukamoto-type four fuzzy reasoning rules containing these fuzzy sets, unknown control inputs updated at various timings are flexibly inferred from known control commands given by the fixed periodical sampled-data controller.

Consequently, the contributions of this research are indicated as follows.

(C1). The variations of updating timings of the control input by the actuator are more explicitly addressed by the Tsukamoto-type

fuzzy-reasoning-based compensation. The proposed approach reflects human-thought-like knowledges (decisions) in the inference mechanism and consists of only four fuzzy rules, resulting in a simpler compensation. Moreover, the proposed intuitive compensation does not require complicated mathematical modeling of the time-varying control cycles.

(C2). Employing a sampled-data controller effectively copes with discretization errors due to implementation of a digital vibration controller with the long control cycle.

(C3). The proposed active damping system is validated via simulation studies employing a drivetrain dynamics model with the control cycle limitation. Multiple simulation examples with various plant conditions confirm that the proposed approach has excellent robustness against not only the control cycle values but also plant parameter variations (i.e., modeling uncertainty).

## 2. Drivetrain dynamics model

### 2.1. Simplified transmissional model

In order to focus on transient vibration phenomena due to an abrupt driving force change and the backlash characteristic, this study employs a dynamics model, which simplifies a real drivetrain mechanism while reproducing only the basic configuration, as a controlled object.

**Fig. 2** indicates the simplified drivetrain model for investigating active vibration control systems. The model configuration is expressed as a three-degrees-of-freedom transmissional oscillation system containing a dead-zone characteristic due to backlash. A driving force  $u$  is transferred between three mass points  $M_E$ ,  $m_G$ , and  $M_B$  via springs and dampers. The model specifications are presented in **Table 2**. In [29–31], more details on the model structure can be found. The driving force  $u$  combined with the control cycle limitation part, which is explained later, plays an actuator's role.

### 2.2. Modeling for vibration controller design

As the drivetrain system has nonlinearities such as the backlash, the linearized model is required for designing a basic damping controller (i.e., sampled-data controller). The time-varying linear state equation and the output equation of the system are then derived as

$$\dot{\mathbf{x}}_p = \mathbf{A}_p \mathbf{x}_p + \mathbf{B}_{p1} \mathbf{w}_p + \mathbf{B}_{p2} u \quad (1)$$

$$\mathbf{y}_p = \mathbf{C}_p \mathbf{x}_p + \mathbf{D}_{p1} \mathbf{w}_p + \mathbf{D}_{p2} u \quad (2)$$

Each coefficient matrix and the state vector are

$$\begin{aligned} \mathbf{A}_p &= \begin{bmatrix} 0 & 0 & 0 & 1 & 0 & 0 \\ 0 & 0 & 0 & 0 & 1 & 0 \\ 0 & 0 & 0 & 0 & 0 & 1 \\ -\frac{(K_D + K_C)}{M_B} & \frac{K_D}{M_B} & 0 & -\frac{(C_D + C_C)}{M_B} & \frac{C_D}{M_B} & 0 \\ \frac{K_D}{m_G} & -\frac{(SwK_G + K_D)}{m_G} & \frac{SwK_G}{m_G} & \frac{C_D}{m_G} & -\frac{(SwC_G + C_D)}{m_G} & \frac{SwC_G}{m_G} \\ 0 & \frac{SwK_G}{M_E} & -\frac{SwK_G}{M_E} & 0 & \frac{SwC_G}{M_E} & -\frac{(SwC_G + C_{el})}{M_E} \end{bmatrix} \\ \mathbf{B}_{p1} &= \begin{bmatrix} 0 & 0 \\ 0 & 0 \\ 0 & 0 \\ 0 & \frac{1}{M_B} \\ \frac{1}{m_G} & 0 \\ -\frac{1}{M_E} & 0 \end{bmatrix}, \mathbf{B}_{p2} = \begin{bmatrix} 0 \\ 0 \\ 0 \\ 0 \\ 0 \\ \frac{1}{M_E} \end{bmatrix}, \mathbf{C}_p = [1 \ 0 \ 0 \ 0 \ 0 \ 0] \end{aligned} \quad (3)$$

$$\mathbf{D}_{p1} = 0, \quad \mathbf{D}_{p2} = 0$$

$$\mathbf{x}_p = [X_B \ X_G \ X_E \ \dot{X}_B \ \dot{X}_G \ \dot{X}_E]^T \quad (4)$$

In Eqs. (1) and (2),  $u$  indicates the control input, and  $\mathbf{w}_p$  is the disturbance including force due to the backlash. The dead-zone effect due to backlash is expressed by switching of the time-varying parameter  $Sw$ . The switching rule is shown below [32,33].  $|\delta|$  is dead

**Table 2**  
Parameters of the drivetrain model.

Parameter	Value	Unit
$M_B$	0.232	kg
$m_G$	0.039	kg
$M_E$	1.04	kg
$K_C$	660.0	N/m
$K_D$	$3.6 \times 10^4$	N/m
$K_G$	$4.2 \times 10^4$	N/m
$C_C$	0.2	Ns/m
$C_D$	15.5	Ns/m
$C_G$	45.0	Ns/m
$C_{cl}$	2.3	Ns/m

zone width and  $F$  is a force via the spring  $K_G$ . When designing a fixed periodical sampled-data controller offline, the value of  $S_w$  is set to be 1.0.

$$F = S_w \cdot K_G \cdot \Delta X + OKG = S_w \cdot K_G \cdot (X_E - x_G) + OKG$$

$$S_w = \begin{cases} 1, & X_E - x_G > |\delta| \\ 1, & X_E - x_G < -|\delta|, \\ 0, & |X_E - x_G| \leq |\delta| \end{cases}, \quad OKG = \begin{cases} -K_G \times |\delta|, & X_E - x_G > |\delta| \\ |K_G \times |\delta||, & X_E - x_G < -|\delta| \\ 0, & |X_E - x_G| \leq |\delta| \end{cases} \quad (5)$$

The time-varying linear state equation of the plant with the backlash and other nonlinear characteristics is also described in [29].

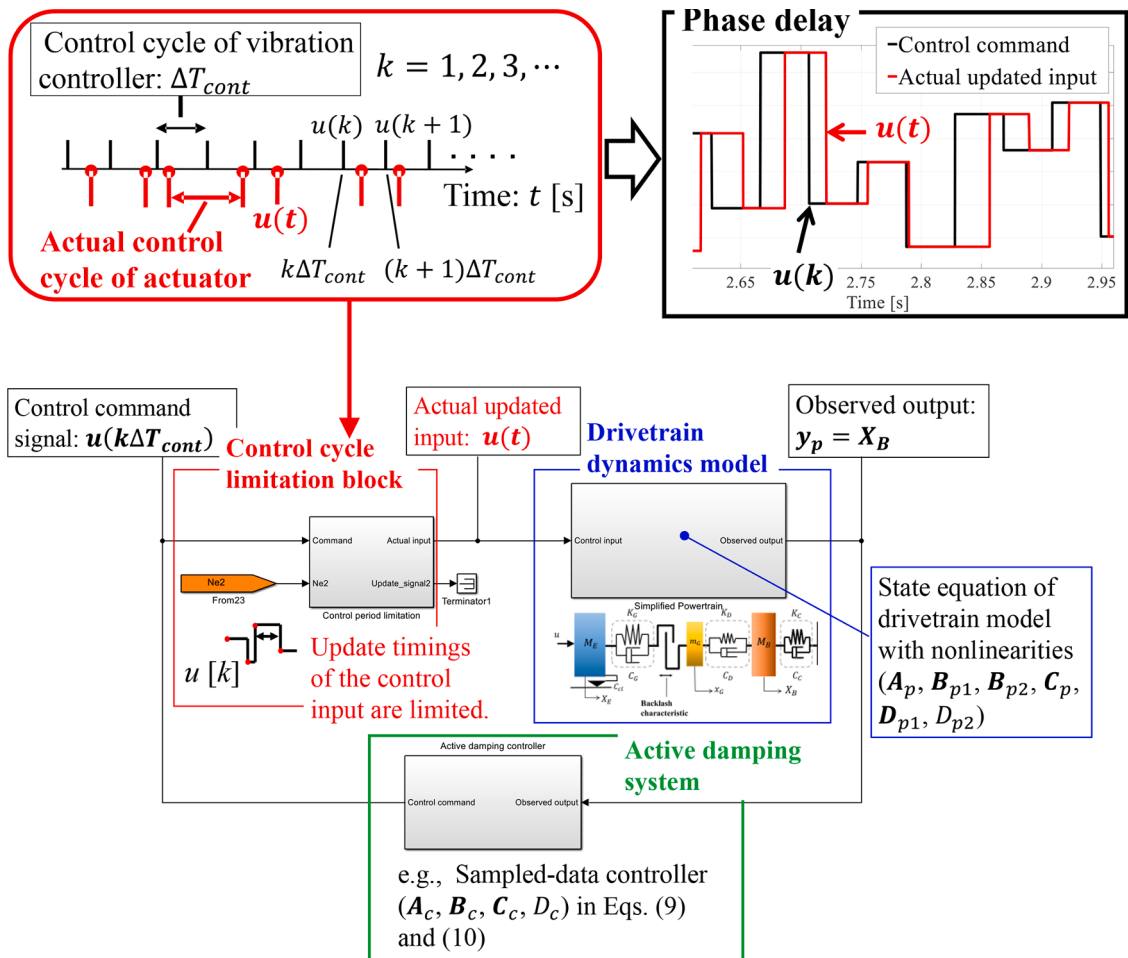


**Fig. 3.** Simulation diagram (Simulink model) consisting of a drivetrain model, a control cycle generation part, and an active damping controller.

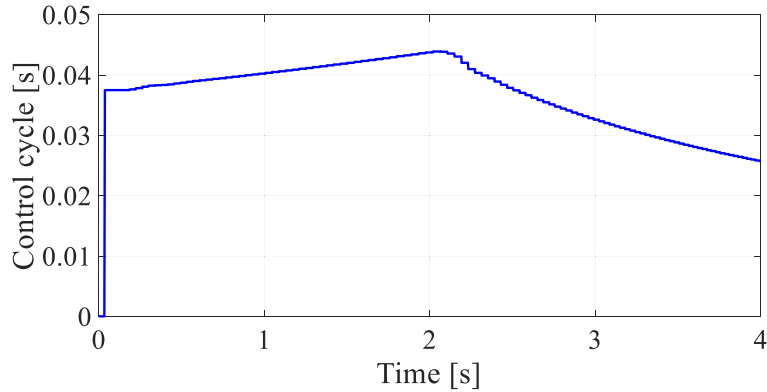


Fig. 4. Time history of the control cycle.

### 3. Time-varying and long control cycle of actuator

#### 3.1. Control cycle limitation in simulation model

In simulation validations, only the control cycle limitation model, which is equivalent to that of an engine, is combined with the above drivetrain dynamics model. Fig. 3 shows the simulation diagram (Simulink model) of a closed-loop system, which consists of the simplified drivetrain model, a control cycle generation part, and an active damping controller.

The time-varying and long control cycles, like those shown in Fig. 4, are generated in the control cycle limitation block. According to these control cycles, the control input, which is actually applied to the latter drivetrain model, is only updated at the limited timings. In Fig. 4, the frequency of actually updating the control input varies from approximately 5.7 to 9.7 times the natural frequency (4 Hz) to be controlled between 2.0 s and 4.0 s.

#### 3.2. Various update timings of control input

As explained in the conceptual diagram of Fig. 5, the problem to be tackled in this paper is the phenomenon that the timing of actually updating the control inputs by the actuator is perturbed from that of an active damping controller executed at a fixed time interval  $\Delta T_{cont}$ . The variation of updating timings of the control input, i.e., time-varying control cycle, results in phase delays of the control input, which considerably degrade vibration suppression performances. Fig. 6 indicates one simulation example of such phase differences.

For the situation shown in Fig. 5, the following question needs to be discussed. If both of the control command values  $u(k)$  at (1)  $t = k\Delta T_{cont}$  and  $u(k+1)$  at (2)  $t = (k+1)\Delta T_{cont}$  have been already given by a fixed periodical vibration controller, the main concern of this paper is what kind of control commands should be given to the actuator within the time zone (3)  $k\Delta T_{cont} < t < (k+1)\Delta T_{cont}$ .

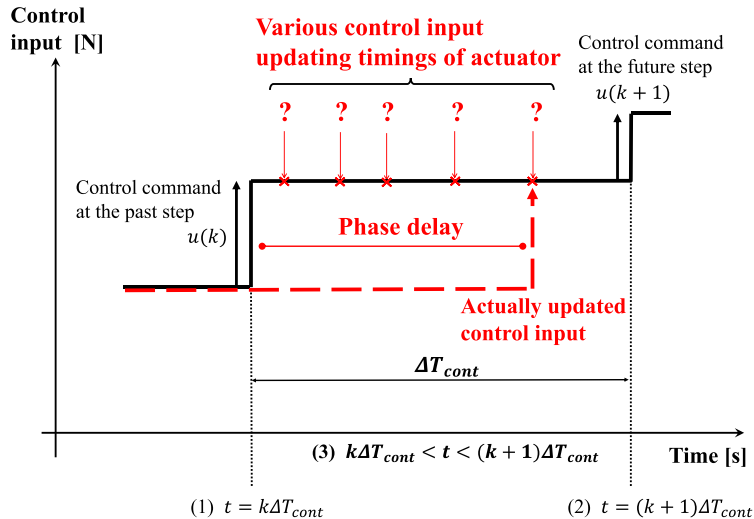
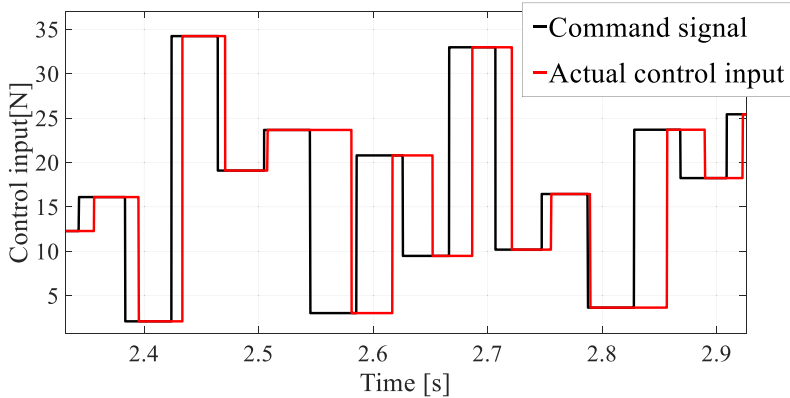


Fig. 5. Variation of updating timings of actual control inputs from those of a fixed periodical vibration controller.



**Fig. 6.** Phase differences between the control input (red line) updated by the actuator and the control command (black line) from a vibration controller.

#### 4. Proposed active vibration suppression system

The entire control logic is composed of two major parts. One is the model predictive processing based on a sampled-data controller [21]. The other is the Tsukamoto-type fuzzy-reasoning-based compensation for various update timings of the control input. Fig. 7 overviews the entire control strategy, representing the conceptual time history of the control command. In Fig. 7,  $u(k)$  and  $u(k+1)$  indicate the control commands computed at (1)  $t = k\Delta T_{cont}$  and at (2)  $t = (k+1)\Delta T_{cont}$ , respectively. They are given by the fixed-periodical sampled-data controller and the model predictive simulation described later. The fuzzy-reasoning-based compensation is applied within (3)  $k\Delta T_{cont} < t < (k+1)\Delta T_{cont}$  to compute proper control commands at various updating timings based on  $u(k)$  and  $u(k+1)$ . The other symbols shown in Fig. 7 are explained later.

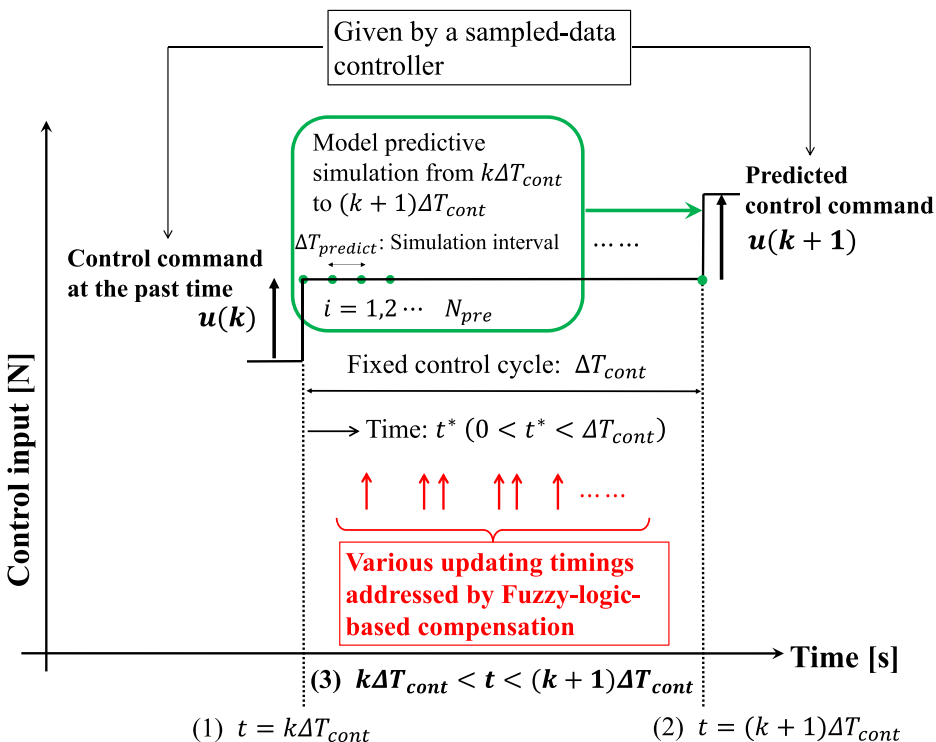


**Fig. 7.** Outline of the proposed active damping strategy.

#### 4.1. Model predictive compensation with sampled-data controller

Because of the long updating intervals of the control input of the actuator, the influences of discretization errors involved with the implementation of a digital vibration controller cannot be neglected. Hence, a sampled-data controller [34–36], which does not require any discretization in its implementation process, becomes the suitable choice to ensure active damping performances [21,30].

Fig. 8(a) shows the block diagram used to design a fixed periodical sampled-data  $H_2$  controller [34–36].

$z_1$  and  $z_2$  indicate the controlled variables, and the vehicle body vibration  $y = X_B$  is a measured output. The gain of each weighting function  $W_i(s)$  ( $i = y, u$ ) is shown in Fig. 8(b). For instance, a transfer function  $W_y(s)$  is written as

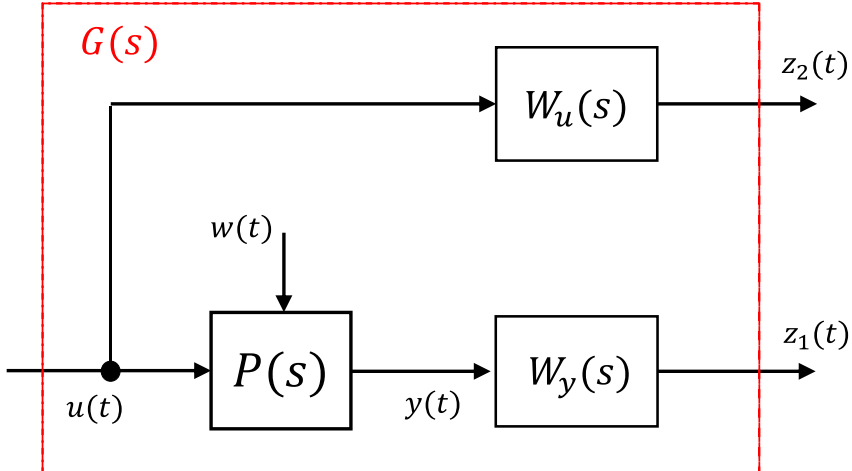
$$M(s) = \frac{s + (2\pi \times \varepsilon_2)}{1.0} \quad (6)$$

$$\tilde{W}_y(s) = \frac{1.984 \times 10^9}{s^3 + 251.3s^2 + 3.158 \times 10^4 s + 1.984 \times 10^6} \times \frac{1.0}{s + (2\pi \times \varepsilon_1)} \quad (7)$$

$$W_y(s) = \tilde{W}_y(s) \cdot M(s) \quad (8)$$

Refer [21] for the detailed selection policies of  $W_y(s)$  and  $W_u(s)$  with the tuning parameters  $\varepsilon_1$  and  $\varepsilon_2$ .

(a)



(b)

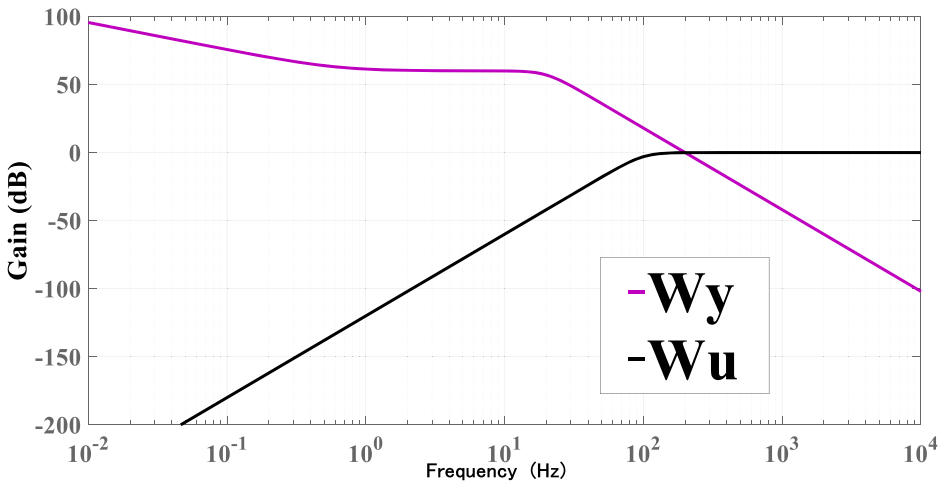


Fig. 8. Design of a sampled-data controller: (a) generalized plant (b) gain of the frequency weighting functions.

The form of the sampled-data  $H_2$  controller, which is derived directly from the continuous-time plant  $P(s)$ , becomes a discrete-time state-space representation as

$$\mathbf{x}_c(k+1) = \mathbf{A}_c \mathbf{x}_c(k) + \mathbf{B}_c(X_B(k\Delta T_{cont}) - r(k\Delta T_{cont})) \quad (9)$$

$$u(k) = \mathbf{C}_c \mathbf{x}_c(k) + D_c(X_B(k\Delta T_{cont}) - r(k\Delta T_{cont})) \quad (10)$$

$r(k\Delta T_{cont})$  is the target signal set as a step response according to tip-in and tip-out conditions of a vehicle.  $\mathbf{x}_c(k)$  indicates the state vector of the sampled-data controller, and  $k$  ( $k = 1, 2, 3, \dots$ ) is the number of calculation steps with respect to the fixed period  $\Delta T_{cont}$  of the sample-data controller. Based on Eqs. (9) and (10) combined with the feedforward input of the target signal [29,30], the control signal  $u(k)$  is commanded at the step  $t = k\Delta T_{cont}$ .

Figs. 5 and 6 demonstrate that the time-varying control cycle results in phase delays of the control input of the actuator. In this subsection, focusing on dealing with the maximal phase delay  $\Delta T_{cont}$ , the model predictive compensation is performed [21]. That is, the information on the future command signal  $u(k+1)$  from the sampled-data controller at  $t = (k+1)\Delta T_{cont}$  can be known at the step  $t = k\Delta T_{cont}$  via the predictive processing, and therefore the phase delay compensation is realized. To approximately derive the future control command  $u(k+1)$ , a real-time simulation of the plant from (1)  $t = k\Delta T_{cont}$  to (2)  $t = (k+1)\Delta T_{cont}$  consisting of  $N_{pre}$  steps (i.e., calculation interval of  $\Delta T_{predict}$ ) is executed as

$$\begin{aligned} \mathbf{x}_{pd}[i+1] &= \mathbf{A}_{pd} \mathbf{x}_{pd}[i] + \mathbf{B}_{p1d} \mathbf{w}_p[i] + \mathbf{B}_{p2d} u[i] \\ &= \{\mathbf{I} + \Delta T_{predict} \cdot \mathbf{A}_p(t)\} \mathbf{x}_{pd}[i] + \{\Delta T_{predict} \cdot \mathbf{B}_{p1}(t)\} \mathbf{w}_p[i] + \{\Delta T_{predict} \cdot \mathbf{B}_{p2}(t)\} u[i] \end{aligned} \quad (11)$$

$$y_{pd}[i] = \mathbf{C}_{pd} \mathbf{x}_{pd}[i] + \mathbf{D}_{p1d} \mathbf{w}_p[i] + D_{p2d} u[i] = \mathbf{C}_p(t) \mathbf{x}_{pd}[i] \quad (12)$$

where

$$i = 1, 2, \dots N_{pre} \quad (13)$$

$$N_{pre} = \frac{\Delta T_{cont}}{\Delta T_{predict}} + 1 \quad (14)$$

Using the time-varying linear state equation of the plant with nonlinearities such as the backlash [29,30], Eqs. (11) and (12) are obtained online. The plant state estimation noted later also utilizes the time-varying linear state equation. In Eqs. (11) and (12),  $u[i]$  is the control input driving the actuator, and  $\mathbf{w}_p[i]$  is the external input including the term due to backlash. The discrete-time coefficient matrices are approximately computed from the continuous-time model.

To obtain initial conditions of the online simulation, the state vector  $\mathbf{x}_{pd}[i]$  is estimated based on the Kalman filtering theory using the time-varying linear state equation [31].

To predict  $u(k+1)$  at  $t = (k+1)\Delta T_{cont}$  in the online simulation, the state equation of the sampled-data controller ( $\mathbf{A}_c$ ,  $\mathbf{B}_c$ ,  $\mathbf{C}_c$ ,  $D_c$ ) with the fixed updating cycle  $\Delta T_{cont}$  can be used.

#### 4.2. Tsukamoto-type fuzzy-reasoning-based compensation for various update timings

This research presents a simple fuzzy-reasoning-based compensation for various control input update timings between  $t = k\Delta T_{cont}$  and  $t = (k+1)\Delta T_{cont}$  (i.e.,  $k\Delta T_{cont} < t < (k+1)\Delta T_{cont}$ ). Below is an outline of the control strategy applied within time zone (3) in Fig. 7.

In the proposed basic idea, the variation of timings at which the control input values are updated by the actuator is expressed as the “fuzziness” against the periodical fixed updating timings (i.e., “future step  $t = (k+1)\Delta T_{cont}$ ” and “past step  $t = k\Delta T_{cont}$ ”) of the control commands of the sampled-data controller. Specifically, the control input updating timing is expressed as the fuzzy sets “Approximately past step  $t = k\Delta T_{cont}$ ”, “Approximately middle step  $t = (k+1/2)\Delta T_{cont}$ ”, and “Approximately future step  $t = (k+1)\Delta T_{cont}$ ”. Furthermore, in order to use the following qualitative human-thought-like knowledge,

(Knowledge 1) “The closer an updating timing of an unknown control input is to  $t = k\Delta T_{cont}$  or  $t = (k+1)\Delta T_{cont}$ , the more similar its control input value will be to  $u(k)$  or  $u(k+1)$ , respectively.”

We also provide fuzziness for the control commands  $u(k)$  at the past step and  $u(k+1)$  at the future step already obtained from the sampled-data controller. Based on all of the factors comprehensively such as “how close various updating timings within  $k\Delta T_{cont} < t < (k+1)\Delta T_{cont}$  are to the future step”, “how close they are to the past step”, and “how close they are to the middle point”, a reasonable control input can be flexibly inferred from the fuzzy sets “About  $u(k)$ ” and “About  $u(k+1)$ ”.

The magnitude of the time rate of change in control output, that is the velocity vibration  $\dot{y}_p = \dot{X}_B$ , is also considered for the proposed fuzzy inference rules. Specifically, the following qualitative consideration is employed in the fuzzy inference.

(Knowledge 2) “If the control output fluctuates more significantly in the future, the phase delay of the control input will have adverse effects more considerably. Therefore, for that situation, employing the predicted control input  $u(k+1)$  is more suitable for the phase-delay compensation (i.e., employing the control input computed at the past step is more unsuitable).”

Consequently, the fuzzy if-then inference rules (15)–(18) are proposed in this study. In (15)–(18), the input variable  $t$  is time within  $k\Delta T_{cont} < t < (k+1)\Delta T_{cont}$ , and the output variable  $u(t)$  represents the control input at that time.

(Rule 1).

IF ( $t$  is about  $(k+1)\Delta T_{cont}$ ) THEN ( $u(t)$  is about  $u(k+1)$ ) (15)

(Rule 2).

IF ( $t$  is about  $k\Delta T_{cont}$ ) THEN ( $u(t)$  is about  $u(k)$ ) (16)

(Rule 3).

IF  $\left(t \text{ is about } \left(k + \frac{1}{2}\right)\Delta T_{cont}\right)$  and  $(|\dot{y}_p| \text{ is Big})$  THEN ( $u(t)$  is about  $u(k+1)$ ) (17)

(Rule 4).

IF  $\left(t \text{ is about } \left(k + \frac{1}{2}\right)\Delta T_{cont}\right)$  and  $(|\dot{y}_p| \text{ is Small})$  THEN ( $u(t)$  is about  $u(k)$ ) (18)

The reason why (Rule 1) is necessary is because the above-mentioned (Knowledge 1) needs to be applied to  $u(k+1)$  already computed at  $t = (k+1)\Delta T_{cont}$ . Specifically, the following knowledge, “If an unknown control input is updated at timings near to  $t = (k+1)\Delta T_{cont}$ , its proper value should be similar to  $u(k+1)$ ”, must be reflected in the proposed inference mechanism. That is, (Rule 1) plays a role of applying this knowledge to various control input updating timings within  $k\Delta T_{cont} < t < (k+1)\Delta T_{cont}$ . In the same way, the reason why (Rule 2) is necessary is because (Knowledge 1) needs to be applied to  $u(k)$  already computed at  $t = k\Delta T_{cont}$ .

Because Rules 1 and 2 contribute to deriving the proper fuzzy output updated at timings near to  $t = (k+1)\Delta T_{cont}$  and  $t = k\Delta T_{cont}$ , respectively, both of them must exist to deal with various updating timings within  $k\Delta T_{cont} < t < (k+1)\Delta T_{cont}$ . The absence of either one of the two rules makes the inference ensuring the fundamental control performance impossible.

The reason why (Rule 3) and (Rule 4) are necessary is because the above-mentioned (Knowledge 2) needs to be considered in the inference process. It is required to give another information for inference of the control input that is updated just in the middle between  $t = k\Delta T_{cont}$  and  $t = (k+1)\Delta T_{cont}$ . As the timing  $t = (k+1/2)\Delta T_{cont}$  is exactly neutral to both  $t = k\Delta T_{cont}$  and  $t = (k+1)\Delta T_{cont}$ , whether  $u(k)$  or  $u(k+1)$  is more appropriate cannot be judged from timing alone. Rules 3 and 4 contribute to determining how much the effect of the phase delay compensation should be used. This decision is based on not only timings but also the vehicle body vibration.

If Rules 3 and 4 are not included in the inference scheme, the process of deriving the fuzzy output becomes too rough because actual vehicle body responses are not directly reflected in the inference process.

The following part gives the specific reasoning processes. This research employs Tsukamoto-type fuzzy reasoning [37–39] because of its high computation efficiency. To make the rules (15)–(18) more suitable form for the reasoning, they are translated into the equivalent rules (19)–(22). Here,  $t^*$  is defined as  $t^* = t - k\Delta T_{cont}$  within  $0 < t^* < \Delta T_{cont}$ .

(Rule 1).

IF( $t^*$  is about future( $\Delta T_{cont}$ ))THEN( $u(t^*)$  is about  $u(k+1)$ ) (19)

(Rule 2).

IF ( $t^*$  is about past(0))THEN ( $u(t^*)$  is about  $u(k)$ ) (20)

(Rule 3).

IF  $\left(t^* \text{ is about middle}\left(\frac{1}{2}\Delta T_{cont}\right)\right)$  and  $(|\dot{y}_p| \text{ is Big})$  THEN ( $u(t^*)$  is about  $u(k+1)$ ) (21)

(Rule 4).

IF  $\left(t^* \text{ is about middle}\left(\frac{1}{2}\Delta T_{cont}\right)\right)$  and  $(|\dot{y}_p| \text{ is Small})$  THEN ( $u(t^*)$  is about  $u(k)$ ) (22)

**Table 3** summarizes the above inference rules (i.e., Rules 1–4) in (19)–(22). The total number of the fuzzy rules required is four. The symbol “–” in **Table 3** means that the fuzzy sets and rules are not defined.

As written in Eqs. (23)–(27), the fuzzy sets “about future ( $\Delta T_{cont}$ )”, “about past (0)”, and “about middle ( $\frac{1}{2}\Delta T_{cont}$ )” are expressed as the membership functions  $h_{future}^t$ ,  $h_{past}^t$ , and  $h_{middle}^t$ , respectively. “Big” and “Small” are defined by  $h_{Big}^{CY}$  and  $h_{Small}^{CY}$ , respectively. Fig. 9 (a)

**Table 3**

Tsukamoto-type fuzzy rule table of Rules 1–4 in (19)–(22) (input variables:  $t^*$  and  $|\dot{y}_p|$ , output variable:  $u(t^*)$ ).

$t^* = t - k\Delta T_{cont}$ within $0 < t^* < \Delta T_{cont}$ .				
	“About future ( $\Delta T_{cont}$ )”	“About past (0)”	“About middle ( $\frac{1}{2}\Delta T_{cont}$ )”	
$ \dot{y}_p  \geq 0$ (Maximal value: $ \dot{y}_p _{max}$ )	–	“About $u(k+1)$ ”	“About $u(k)$ ”	–
“Big”	–	–	–	“About $u(k+1)$ ”
“Small”	–	–	–	“About $u(k)$ ”

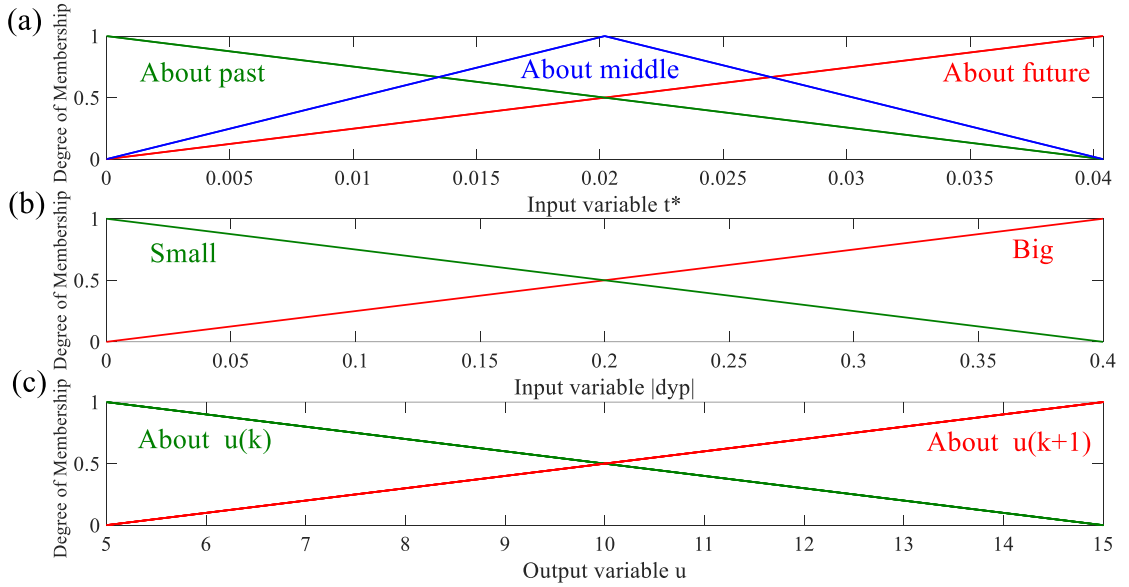


**Fig. 9.** Membership functions for (a) input variable  $t^*$ , (b) input variable  $|\dot{y}_p|$ , and (c) output variable  $u$ .

and (b) show numerical examples of the membership functions for the input variables  $t^*$  and  $|\dot{y}_p|$ .

$$h_{future}^t = \frac{1}{\Delta T_{cont}} \cdot t^* \quad (23)$$

$$h_{past}^t = -\frac{1}{\Delta T_{cont}} \cdot t^* + 1 \quad (24)$$

$$h_{middle}^t = \frac{2}{\Delta T_{cont}} \left( - \left| t^* - \frac{1}{2} \Delta T_{cont} \right| + \frac{1}{2} \Delta T_{cont} \right) \quad (25)$$

$$h_{Big}^{cy} = \frac{1}{|\dot{y}_p|_{max}} \cdot |\dot{y}_p| \quad (26)$$

$$h_{Small}^{cy} = -\frac{1}{|\dot{y}_p|_{max}} \cdot |\dot{y}_p| + 1 \quad (27)$$

Here,  $|\dot{y}_p|_{max}$  in Eqs. (26) and (27) represents the maximal value, that is a tuning parameter for  $h_{Small}^{cy}$  and  $h_{Big}^{cy}$ , in the input space of  $|\dot{y}_p|$ . Other points above  $|\dot{y}_p|_{max}$  are mapped to a membership value of 1 or 0.

The membership functions  $h_{future}^t$ ,  $h_{past}^t$ , and  $h_{middle}^t$  are required to provide fuzziness for the three timings,  $(k+1)\Delta T_{cont}$  (i.e.,  $\Delta T_{cont}$  for  $t^*$ ),  $k\Delta T_{cont}$  (i.e., 0 for  $t^*$ ), and  $(k+1/2)\Delta T_{cont}$  (i.e.,  $1/2\Delta T_{cont}$  for  $t^*$ ), respectively. Because the sampled-data controller updates the control commands at the fixed time interval  $\Delta T_{cont}$ , the two fixed timings  $(k+1)\Delta T_{cont}$  and  $k\Delta T_{cont}$  need to be considered. In addition, from the above reason, the middle time point  $(k+1/2)\Delta T_{cont}$  is additionally considered. Consequently, the total number of required membership functions for  $t^*$  is three. The range  $[0, \Delta T_{cont}]$  is also the calculation period of the sampled-data controller. Therefore,  $\Delta T_{cont}$  needs to be determined according to the sampled-data controller tuning. It is desirable to set  $\Delta T_{cont}$  as long as possible considering the time-varying control cycle.

The combination of the sampled-data controller and the fuzzy logic has the robustness against control cycle variations. Hence, the proper fuzzy output can be still derived even with some fluctuated  $\Delta T_{cont}$ .

The membership functions  $h_{Big}^{cy}$  and  $h_{Small}^{cy}$  are required to express the two fuzzy sets "Big" and "Small", respectively. Because the application of only a small number of the fuzzy rules and membership variables contributes to realizing the simpler configuration, only the two levels "Big" and "Small" are employed with respect to  $|\dot{y}_p|$ .

The range  $[0, |\dot{y}_p|_{max}]$  needs to be manually tuned according to the actual vehicle body response. Too large values of  $|\dot{y}_p|_{max}$  reduce the influences of Rule 3 on the fuzzy output because the degree of match for Rule 3 becomes small.

Given the current time of executing inference  $t^*$  and the rate of change in the amount of control output  $|\dot{y}_p|$ , the degree of match  $w_1 \sim w_4$  ( $0 \leq w_i \leq 1, i = 1 \sim 4$ ) of each fuzzy rule is computed as follows.

$$w_1 = h_{future}^t(t^*) \quad (28)$$

$$w_2 = h_{past}^t(t^*) \quad (29)$$

$$w_3 = \min(h_{middle}^t(t^*), h_{Big}^{cy}(|\dot{y}_p|)) \quad (30)$$

$$w_4 = \min(h_{middle}^t(t^*), h_{Small}^{cy}(|\dot{y}_p|)) \quad (31)$$

The output of each fuzzy rule is derived based on the fuzzy sets “about  $u(k+1)$ ” and “about  $u(k)$ ”, which are described by the membership functions  $h_{future}^u$  and  $h_{past}^u$ , respectively. As shown in Eqs. (32)–(37), Tsukamoto-type fuzzy reasoning [37–39] uses monotone decreasing or increasing functions. Depending on whether  $u(k)$  or  $u(k+1)$  is higher, the definition of the membership functions becomes one of the two cases (Case 1) and (Case 2). Fig. 9 (c) indicates just numerical examples of  $h_{future}^u$  and  $h_{past}^u$  for (Case 1). Actually, the values on the horizontal axis in Fig. 9 (c) vary in real time.

(Case 1).  $u(k) < u(k+1)$

$$h_{future}^u = \frac{1}{\Delta u}(u - u(k)) \quad (32)$$

$$h_{past}^u = -\frac{1}{\Delta u}(u - u(k)) + 1 \quad (33)$$

$$\Delta u = u(k+1) - u(k) \quad (34)$$

(Case 2).  $u(k+1) < u(k)$

$$h_{future}^u = -\frac{1}{\Delta u}(u - u(k+1)) + 1 \quad (35)$$

$$h_{past}^u = \frac{1}{\Delta u}(u - u(k+1)) \quad (36)$$

$$\Delta u = u(k) - u(k+1) \quad (37)$$

The membership functions  $h_{future}^u$  and  $h_{past}^u$  are required to express the fuzzy sets “About (Approximately)  $u(k+1)$ ” and “About (Approximately)  $u(k)$ ”, respectively. From the sampled-data controller,  $u(k)$  and  $u(k+1)$  can be automatically computed at  $t = k\Delta T_{cont}$  and  $t = (k+1)\Delta T_{cont}$ , respectively. In addition, a consequent part must use monotonically increasing or decreasing functions according to Tsukamoto-type inference method [37–39]. Therefore, only the two membership functions of “About (Approximately)  $u(k)$ ” and “About (Approximately)  $u(k+1)$ ” are required.

Note that  $u(k)$  and  $u(k+1)$  are not tuning parameters to be manually defined by designers. The sampled-data controller provides  $u(k)$  and  $u(k+1)$  online at the fixed time interval  $\Delta T_{cont}$ , and then the range  $[u(k), u(k+1)]$  or  $[u(k+1), u(k)]$  is automatically determined.

In the Tsukamoto-type fuzzy reasoning, the inference result  $u_i$  ( $i = 1 \sim 4$ ) from each rule is computed based on the degree of match of each fuzzy rule  $w_i$  ( $i = 1 \sim 4$ ) and an inverse function of  $h_{future}^u(u)$  or  $h_{past}^u(u)$  as follows:

(Case 1).  $u(k) < u(k+1)$

$$u_1 = h_{future}^{u-1}(w_1) = u(k) + w_1 \Delta u \quad (38)$$

$$u_2 = h_{past}^{u-1}(w_2) = u(k) - (w_2 - 1) \Delta u \quad (39)$$

$$u_3 = h_{future}^{u-1}(w_3) = u(k) + w_3 \Delta u \quad (40)$$

$$u_4 = h_{past}^{u-1}(w_4) = u(k) - (w_4 - 1) \Delta u \quad (41)$$

**Table 4**  
Parameters for simulation setting.

Properties	Value
$\Delta T_{cont}$ [s]	0.0404 s
$\Delta T_{predict}$ [s]	$2.0 \times 10^{-5}$ s
$ \dot{y}_p _{max}$ [m/s]	0.4 m/s
$\epsilon_1$ [Hz]	$10^{-9}$ Hz
$\epsilon_2$ [Hz]	0.6 Hz
Plant parameter variation	$\pm 10\%$

(Case 2).  $u(k+1) < u(k)$

$$u_1 = h_{future}^{u-1}(w_1) = u(k+1) - (w_1 - 1)\Delta u \quad (42)$$

$$u_2 = h_{past}^{u-1}(w_2) = u(k+1) + w_2\Delta u \quad (43)$$

$$u_3 = h_{future}^{u-1}(w_3) = u(k+1) - (w_3 - 1)\Delta u \quad (44)$$

$$u_4 = h_{past}^{u-1}(w_4) = u(k+1) + w_4\Delta u \quad (45)$$

Then, the final inference result  $u_{Fuzzy}(t)$  from the entire inference system is given as a weighted average of  $u_i$  ( $i = 1 - 4$ ) by each degree of match  $w_i$  ( $i = 1 - 4$ ) as

$$u_{Fuzzy}(t) = \frac{\sum_{i=1}^4 w_i u_i}{\sum_{i=1}^4 w_i} \quad (46)$$

In the time-zone (3)  $k\Delta T_{cont} < t < (k+1)\Delta T_{cont}$  in Fig. 7,  $u_{Fuzzy}(t)$  is employed as the control command signal from the proposed active vibration control system.

## 5. Validation of the active vibration control system

### 5.1. Simulation settings

The simulation study is aimed at validating the effectiveness of the proposed active damping system as well as the robustness against various conditions of the drivetrain dynamics. The purpose of the control scheme is to suppress the vehicle body oscillation  $X_B$ , resulting in realization of an ideal step target signal. Considering the driving situation of real vehicles such as tip-in/tip-out, this ideal response smoothly changes from a negative value to a positive value at 2.0 s.

In the simulation verifications, the proposed approach is compared with two other previous damping controllers. One is use of only a sampled-data  $H_2$  controller without any compensations. The other is the model predictive approach that its basic concept was proposed in the previous paper [21]. The parameters for simulation setting are indicated in Table 4.

### 5.2. Results and discussion

As shown in the upper graph of Fig. 10 of the simulation result (“Case No. 0” in Table 5), the proposed method indicated in the red line achieves the highest vibration control performance. The comparisons with the use of only a sampled-data  $H_2$  controller (cyan line) and the previous model predictive approach (blue line) reveal the effectiveness of the proposed fuzzy reasoning rules.

In this paper, Fig. 10 is a representative test result to indicate the fundamental performance of each method. As a quantitative performance evaluation index, the 2-norm of the control error between the target signal (the ideal response shown in the green line) and each vibration response is introduced. In Fig. 10, the 2-norm by the proposed method is reduced by 27.8%, 66.1%, and 66.9% compared to “Predictive control”, “No compensation”, and “Open-loop”, respectively. These results prove that the proposed four fuzzy reasoning rules can compute proper control commands despite the presence of the time-varying control cycle.

The enlarged graph of the control commands given by the proposed active damping system is shown in Fig. 11. The green line indicates the command signal  $u(k)$  computed by the sampled-data controller at the fixed time interval  $\Delta T_{cont}$ . The magenta line represents the value of  $u(k+1)$  that is predicted at the step  $t = k\Delta T_{cont}$  by the model predictive processing. The black line indicates the control command given by the fuzzy rules. The red line indicates the control input actually updated by the actuator.

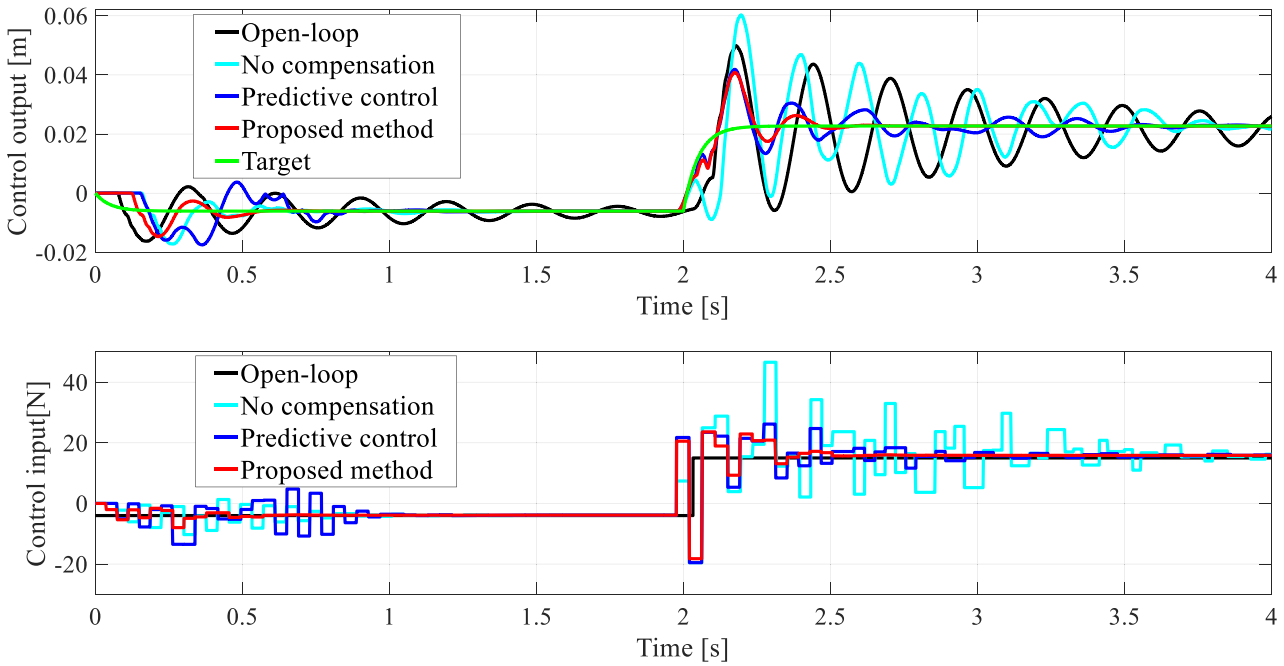


**Fig. 10.** Vehicle body responses and control inputs in the simulation result (Case No. 0).

**Table 5**

Plant parameter variation provided for the controlled object.

Parameter	Nominal Value	Variation amount [%] (Case No. 0)	Variation amount [%] (Case No. 1)	Variation amount [%] (Case No. 2)
$M_B$ [kg]	0.232	0	10	-10
$m_C$ [kg]	0.039	0	-10	10
$M_F$ [kg]	1.04	0	-10	10
$K_C$ [N/m]	660.0	0	10	-10
$K_D$ [N/m]	$3.6 \times 10^4$	0	10	-10
$K_G$ [N/m]	$4.2 \times 10^4$	0	-10	10
$C_C$ [Ns/m]	0.2	0	-10	10
$C_D$ [Ns/m]	15.50	0	10	-10
$C_G$ [Ns/m]	45.0	0	-10	10
$C_d$ [Ns/m]	2.3	0	10	-10

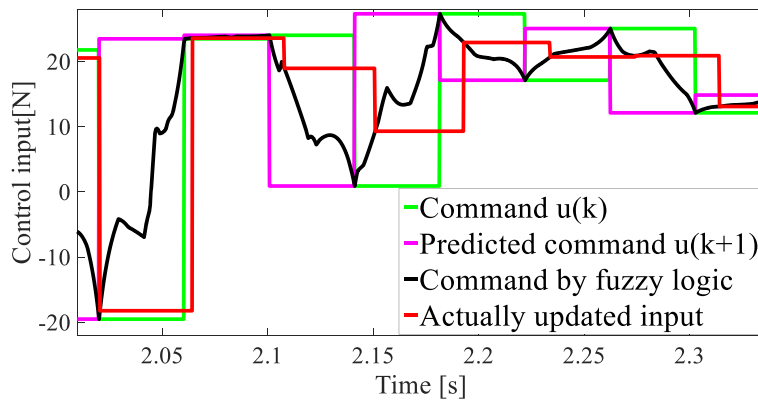


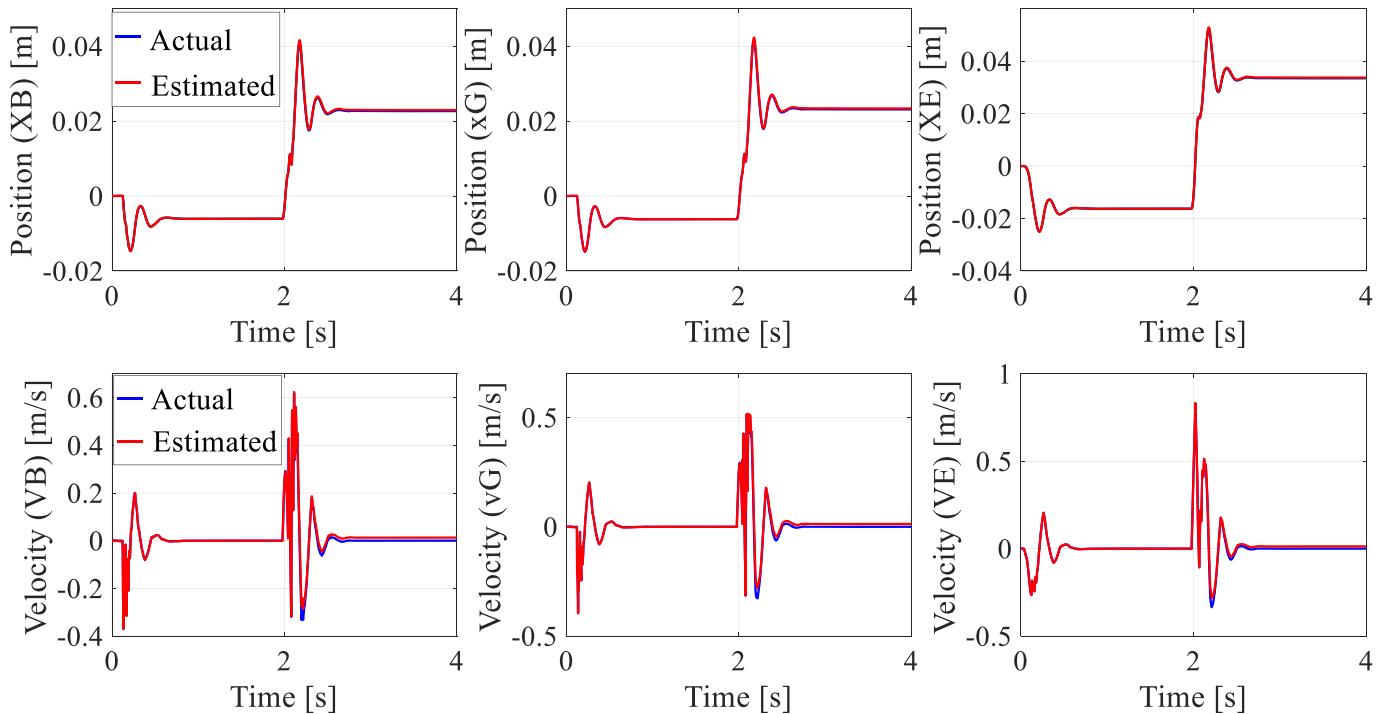
Fig. 11. Enlarged plot of the control commands obtained by the proposed approach.

The command value  $u(k)$  of the green line tracks the predicted value one step ahead  $u(k+1)$  of the magenta line in every step. This tendency in which they match each other by one step reveals a good accuracy of the predictive processing, resulting in proper fuzzy control commands shown in the black line. Fig. 11 demonstrates that the black line continuously varies from a value similar to  $u(k)$  (green line) to a value similar to  $u(k+1)$  (magenta line) in every step. This gradual behavior is given by the fuzzy reasoning rules. Even though the actual control input indicated in the red line is updated at the various timings in Fig. 11, the high damping performance in Fig. 10 is realized by the proposed approach.

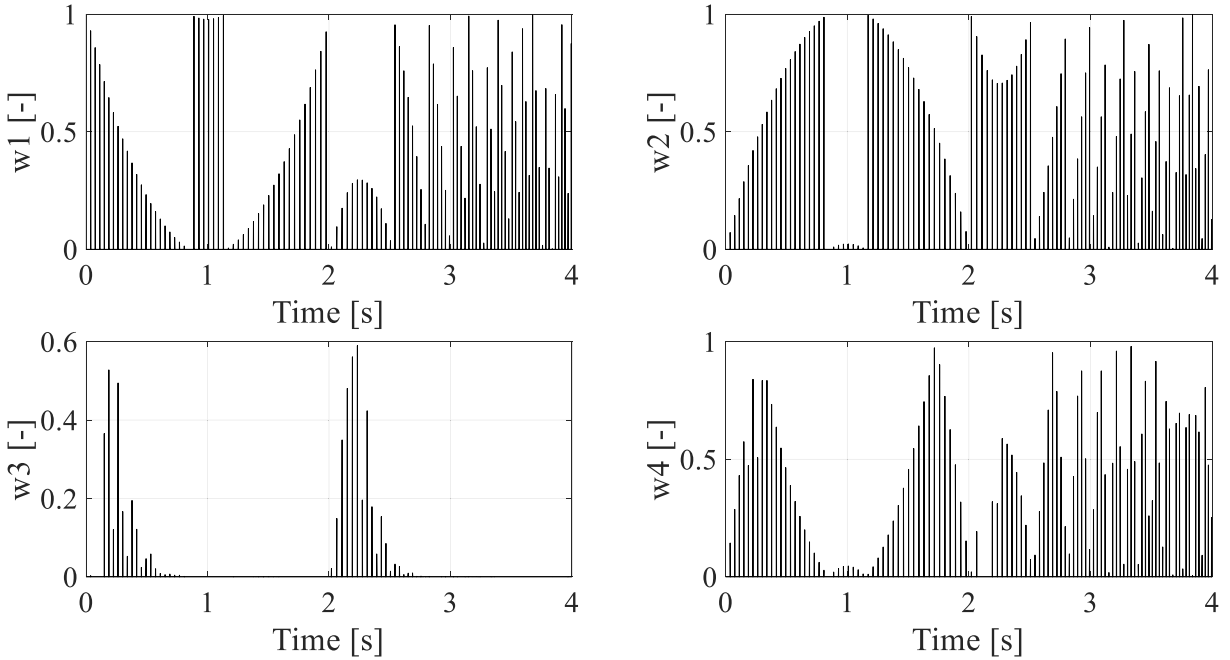
The sufficient state estimation performance, as shown in Fig. 12, is one of required conditions for the successful model-predictive processing. In Fig. 12, the red and blue lines indicate the estimated and actual values of the components of the state vector in Eq. (4), respectively. Each graph in which the red and blue lines almost match each other indicates the high estimation accuracy. In particular, the lower three graphs demonstrate that the velocity responses fluctuating immediately after crossing in backlash are also estimated in the red lines. This is due to use of the time-varying linear state equation including the backlash model [21,31].

Fig. 13 shows the time histories of  $w_i$  ( $i = 1 - 4$ ) at each updating timing. These results demonstrate how much each fuzzy rule contributes to the fuzzy output  $u_{Fuzzy}(t)$  in real time. It can be seen that the large values of  $w_3$  exhibited immediately after the driving force changes (i.e., 2.0 s) contribute to improvement of the transient response. In contrast, the values of  $w_3$  become almost zero after 3.0 s since the vehicle body vibration is already settled (i.e., no fluctuation of the response).

The good control performance in Fig. 10 means that the fusion of Rules 1-4 performed according to  $w_i$  ( $i = 1 - 4$ ) indicated in Fig. 13 gives a suitable control command at various updating timings.



**Fig. 12.** The estimation results for the plant state variables by the Kalman filtering.



**Fig. 13.** Time history of the degree of match of each fuzzy rule.

### 5.3. Verification of robustness against plant parameter variations

Figs. 14 and 15 show the simulation results where variations are provided for the plant parameters. The patterns of the plant parameter variations are listed in Table 5, and the Case No. 1 and 2 correspond to Figs. 14 and 15, respectively. Note that the active damping controllers are designed using the nominal parameters in Table 2. Moreover, a uniformly distributed noise of 10% is added to the observed output used for the state estimation.

For Fig. 14, the cyan line indicates that the combination of the time-varying control cycle and plant parameter variations often results in instability. In the blue line, the residual oscillation as well as the large overshoot immediately after 2.0 s is induced by the combination although the instability is avoided, indicating the limitation of the model predictive compensation. On the other hand, the red line shows the high damping effect that the transient oscillation is quickly converged by about 2.5 s with smaller overshoot. Hence, the robustness of the proposed active damping strategy is clearly seen.

Fig. 15 indicates that completely suppressing the oscillations is difficult for only use of the sampled-data controller or the previous model predictive approach when the plant has uncertainty. The oscillations shown in the cyan and blue lines remain even after 2.5 s although they are not as drastic as Fig. 14. In contrast, the red line still presents the robust performance approximately same as those in Figs. 10 and 14, implying that the proposed method can be applied to several patterns of the plant parameter variations.

Even though there are the modeling errors with respect to uncertainty on the plant parameters, the proposed method maintains excellent transient characteristic, which is approximately the same as that in Fig. 10. In Figs. 14 and 15, the comparisons with the cyan and blue lines imply that the high robustness in the proposed method originates from the application of fuzzy logic. That is, the fuzzy reasoning process may assuage influences due to the modeling errors included in the sampled-data controller or model predictive processing.

Table 6 summarizes the results of additional simulation tests performed based on the result of Fig. 14. In the verifications shown in Table 6, the control performance of each method was investigated when model variations (plant parameter variation and observation noise) other than the above-mentioned 10% variation are given. Regarding the conventional two other methods “No compensation” and “Predictive control”, significant degradation of the control performance of each method was confirmed in 5% and 16% variations, respectively. Specifically, the transient oscillations with greater amplitudes than the open-loop response appeared, and the responses were hardly converged. Compared to the other methods, in 25% variation, the proposed method still maintained a better transient response in which much more amplitude was suppressed, and the transient oscillation was well converged although some residual vibration and a slight decrease in the damping effects were observed.

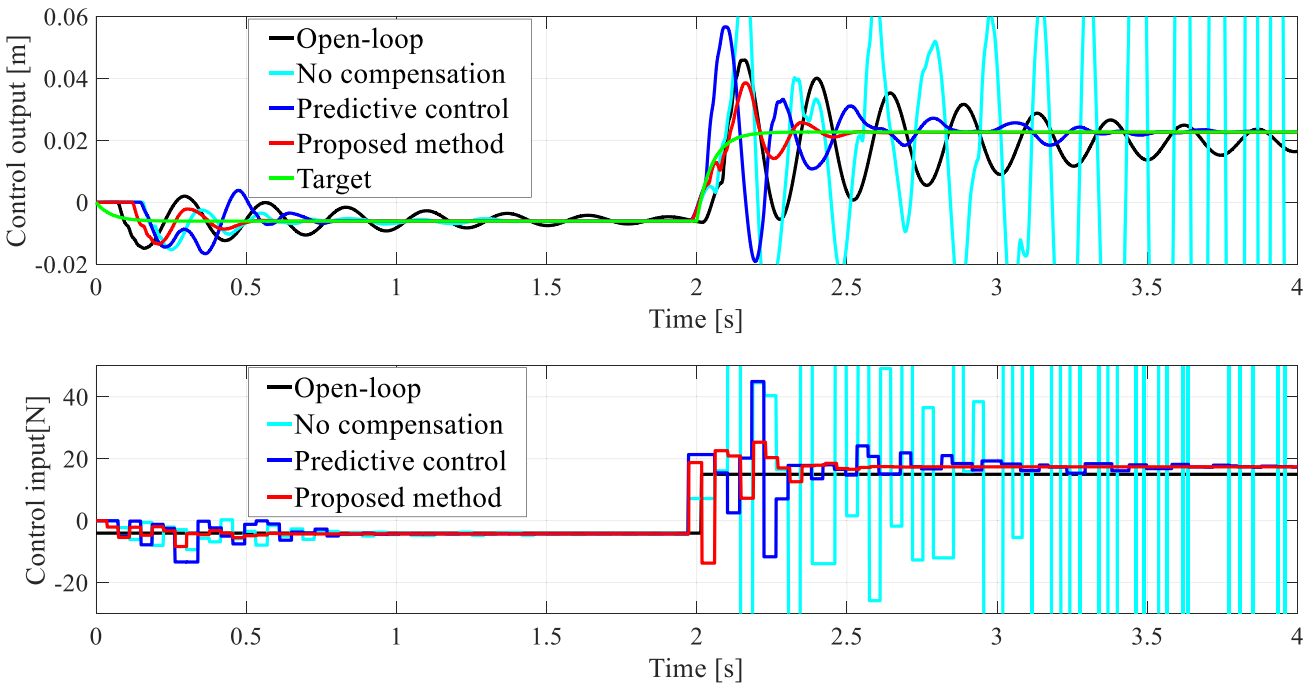


Fig. 14. Vehicle body responses and control inputs in the simulation result with plant parameter variation (Case No. 1).

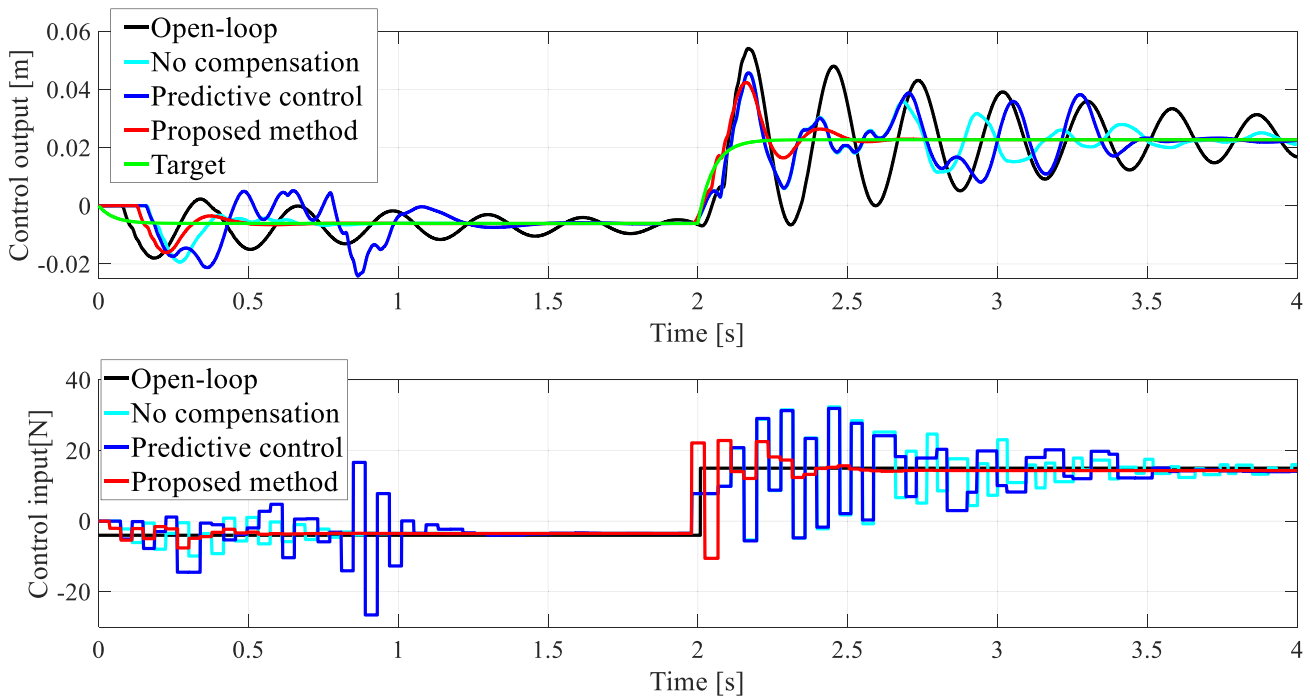
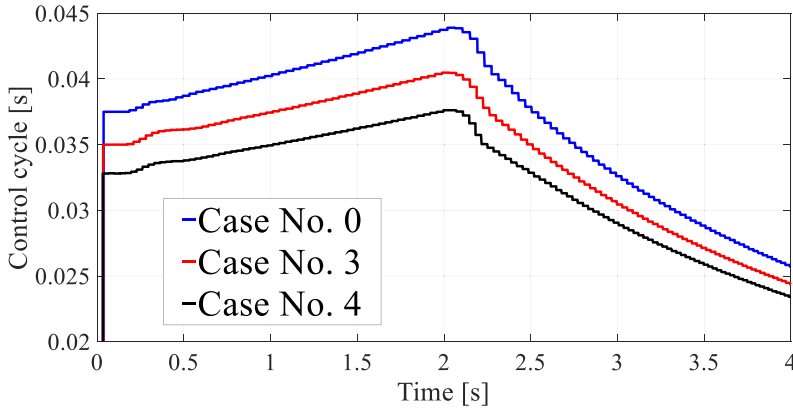


Fig. 15. Vehicle body responses and control inputs in the simulation result with plant parameter variation (Case No. 2).

**Table 6**

Comparison between the three methods based on values of the plant parameter variation and noise.

	Proposed method(With the fuzzy-logic-based compensation)	No compensation(Only a sampled-data controller)	Predictive control(Only the model predictive compensation)
Values of the plant parameter variation and noise	25% variation	5% variation	16% variation

**Fig. 16.** Changes of variable regions of the time-varying control cycle.

#### 5.4. Verification of robustness against variable regions of control cycle

As shown in Fig. 16, another simulation study provides variations for not only the plant parameters, but also the peak value (i.e., variable regions) of the time-varying control cycles. The verification conditions Cases No. 3 and 4 of the two additional variable regions are shown in the red and black lines, respectively, in Fig. 16.

Figs. 17 and 18 show the simulation examples with the changes of the variable regions of the time-varying control cycle. The patterns “Case No. 3” and “Case No. 4” indicated in Fig. 16 correspond to the results of Figs. 17 and 18, respectively.

In Fig. 17, the red and blue lines exhibit the good transient responses while the cyan line still has the residual vibration. This result means necessity of including the predictive processing in the damping strategy. The previous approach [21] should be effective for some patterns of the combinations of the time-varying control cycles and plant parameter variations.

However, Fig. 18 presents a pattern where there is a limitation of the robustness of the previous model predictive processing. The blue line as well as the cyan line is drastically deteriorated, demonstrating that the oscillations are hardly reduced. Nevertheless, the response shown in the red line is quickly settled by 2.5 s with approximately no residual oscillations. Because the fuzzy-reasoning-based compensation proposed in this study is independent of detailed models of the time-varying control cycle, it is free from the variation effects, resulting in the high robustness. The fuzzy logic enables such model-free compensation mechanism.

The comparison results between the three methods clearly seen in Figs. 14, 15, 17 and 18 demonstrate that the proposed approach has excellent robustness against the control cycle values as well as plant parameter variations. For Fig. 17, compared with the cyan line, the improved transient responses of the red and blue lines are due to the phase delay compensations. Nevertheless, the deteriorated responses of the blue line in Figs. 14, 15, and 18 imply that the robustness of the previous model predictive approach may sometimes be poor. This is because dealing with various update timings of the control input within  $k\Delta T_{cont} < t < (k+1)\Delta T_{cont}$  is not explicitly considered [21]. On the other hand, the consistent tendency of the red line across Figs. 14, 15, 17 and 18 demonstrates that the application of fuzzy logic to this compensation can realize robustness against incomplete modeling of drivetrain dynamics due to the complicated control cycle limitation and plant parameter variations.

Table 7 summarizes the results of additional simulation tests performed based on the result of Fig. 17. In 14% variation, “Predictive control” failed to maintain a sufficient damping performance like that in Fig. 17 with 10% variation. In 15% variation, “No compensation” showed deterioration of the damping performance. In 20% variation, the proposed method still exhibited a better transient response that the vibration was quickly converged than the other two methods although an overshoot remains.

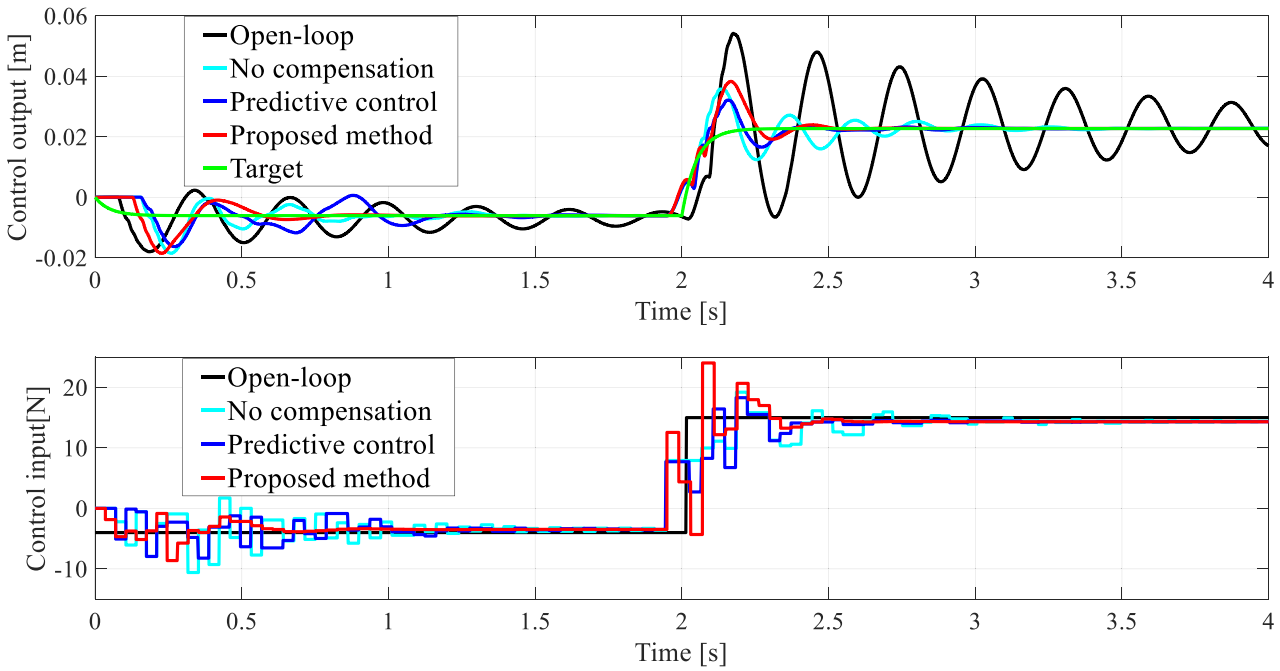
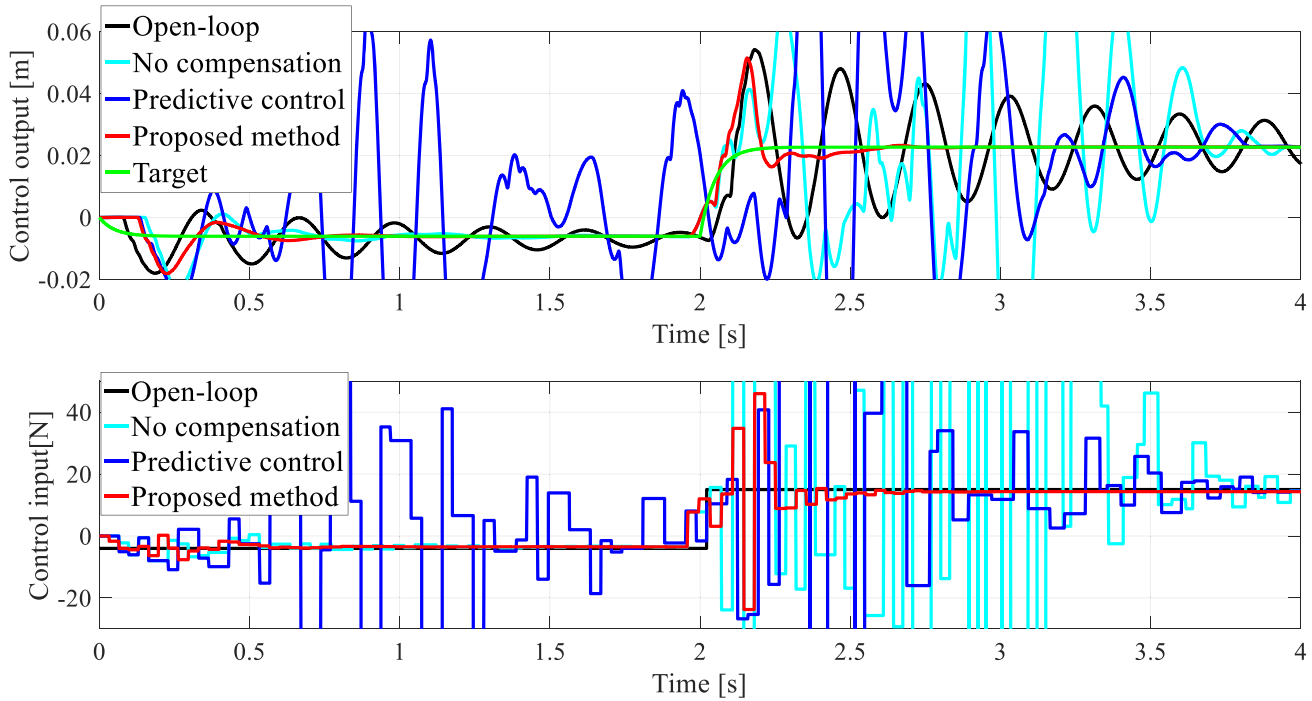


Fig. 17. Vehicle body responses and control inputs in the simulation result with changes of variable regions of the time-varying control cycle (Case No. 3).



**Fig. 18.** Vehicle body responses and control inputs in the simulation result with changes of variable regions of the time-varying control cycle (Case No. 4).

**Table 7**

Comparison between the three methods based on values of the plant parameter variation and noise under change of the variable regions of the control cycle.

	Proposed method(With the fuzzy-logic-based compensation)	No compensation(Only a sampled-data controller)	Predictive control(Only the model predictive compensation)
Values of the plant parameter variation and noise	20% variation	15% variation	14% variation

## 6. Conclusion

For active damping of transient powertrain oscillations using an actuator with the time-varying control cycle limitation, this paper presented the simple fuzzy-reasoning-based compensation algorithm. The simplified drivetrain dynamics model and the simulation configuration with the control cycle limitation were described. The model predictive compensation using a sampled-data controller was applied to tackle the maximal phase delay of the control input due to the time-varying control cycle. The control input updating timing, which is perturbed from that of the fixed periodical controller, was expressed as the fuzzy sets such as “About past step” and “About future step”. Based on those fuzzy sets and known control commands from the sampled-data controller, the Tsukamoto-type fuzzy-reasoning-based compensation was proposed in this research. This can flexibly infer unknown control inputs updated at various timings. The proposed fuzzy compensation explicitly addresses the time-varying control cycle limitation by the simpler configuration with only four intuitive rules and does not involve the complicated modeling. For the representative simulation verification result to indicate the fundamental performance of each method, the 2-norm of the control error by the proposed method was reduced by 27.8%, 66.1%, and 66.9% compared to the previous model predictive approach, only use of the sampled-data control, and open-loop response, respectively. In the verifications with respect to robustness, even though a drivetrain was subject to 10% parameter variations and the control cycles varying in the range between 0.02 s to 0.045 s, the proposed method demonstrated the better transient responses than the other two controls. Moreover, it was revealed that the sufficient damping effect can be maintained even with 25% plant parameter variations and noise.

The limitation of this study is that the proposed method has only been applied to the simplified drivetrain model omitting detailed mechanisms such as other actuator limitations. Therefore, in the future, the proposed controller needs to be applied to a real vehicle powertrain with a more detailed configuration. In addition, the fuzzy rules will be improved to realize more flexible reasoning.

## Funding

A part of this work was supported by Japan Society for the Promotion of Science (JSPS) KAKENHI [Grant Number JP 20J11084].

## Declaration of Competing Interest

The authors declare that they have no known competing financial interests or personal relationships that could have appeared to influence the work reported in this paper.

## References

- [1] A. Scamarcio, P. Gruber, S.D. Pinto, A. Sorniotti, Anti-jerk controllers for automotive applications: a review, *Ann. Rev. Control* 50 (2020) 174–189, <https://doi.org/10.1016/j.arcontrol.2020.04.013>.
- [2] X. Zhang, H. Liu, C. yinqi, Active damping of torsional vibration on the powertrain of power-split vehicle, in: *Energy Proced.*, 105, 2017, pp. 2898–2903.
- [3] C. Lv, J. Zhang, Y. Li, Y. Yuan, Mode-switching-based active control of a powertrain system with non-linear backlash and flexibility for an electric vehicle during regenerative deceleration, *Proc. Inst. Mech. Eng. Part D J. Automob. Eng.* 229 (11) (2015) 1429–1442.
- [4] I.U. Ponce, Y. Orlov, L.T. Aguilar, J. Álvarez, Nonsmooth H<sub>∞</sub> synthesis of non-minimum-phase servo-systems with backlash, *Control Eng. Pract.* 46 (2016) 77–84.
- [5] P. Reddy, M. Shahbakhti, M. Ravichandran, J. Doering, Drivetrain clunk control via a reference governor, *IFAC-PapersOnLine* 54 (20) (2021) 846–851.
- [6] C. Rostiti, Y. Liu, M. Canova, S. Stockar, G. Chen, H. Dourra, M. Prucka, A backlash compensator for drivability improvement via real-time model predictive control, *transactions of the ASME, J. Dyn. Syst. Meas. Control* 140 (10) (2018), 104501.
- [7] A. Formentini, A. Oliveri, M. Marchesoni, M. Storace, A switched predictive controller for an electrical powertrain system with backlash, *IEEE Trans. Power Electron.* 32 (2017) 4036–4047.
- [8] X. Lu, T. Lu, B. Chai, Mode-switch model predictive controller with “pre-contact” method for alleviating driveline vibration of electric vehicles considering backlash, *Proc. Inst. Mech. Eng. Part D J. Automob. Eng.* 234 (8) (2020) 2176–2194.
- [9] O. Atabay, M. Ötkür, İ.M. Ereke, Model based predictive engine torque control for improved drivability, *Proc. Inst. Mech. Eng. Part D J. Automob. Eng.* 232 (12) (2018) 1654–1666.
- [10] C.F. Caruntu, A.E. Balau, M. Lazar, P. Bosch, S.D. Cairano, Driveline oscillations damping: a tractable predictive control solution based on a piecewise affine model, *Nonlinear Anal. Hybrid Syst.* 19 (2016) 168–185.
- [11] M.H. Sarwar, et al., Fuzzy logic-based novel hybrid fuel framework for modern vehicles, *IEEE Access* 8 (2020) 160596–160606, <https://doi.org/10.1109/ACCESS.2020.3010067>.
- [12] M. Awadallah, P. Tawadros, P. Walker, N. Zhang, Dynamic modelling and simulation of a manual transmission based mild hybrid vehicle, *Mech. Mach. Theory* 112 (2017) 218–239, <https://doi.org/10.1016/j.mechmachtheory.2017.02.011>.
- [13] P. Dong, S. Wu, W. Guo, X. Xu, S. Wang, Y. Liu, Coordinated clutch slip control for the engine start of vehicles with P2-hybrid automatic transmissions, *Mech. Mach. Theory* 153 (2020) 103899, <https://doi.org/10.1016/j.mechmachtheory.2020.103899>.
- [14] G. Sun, D. Sun, K. Ma, Y. Kan, J. Shi, Analysis and control of engine starting process based on a novel single-motor power-reflux hybrid electric vehicle, *Mech. Mach. Theory* 168 (2022) 104616, <https://doi.org/10.1016/j.mechmachtheory.2021.104616>.

- [15] D. Lefebvre, P. Chevrel, S. Richard, An H-infinity-based control design methodology dedicated to the active control of vehicle longitudinal oscillations, *IEEE Trans. Control Syst. Technol.* 11 (6) (2003) 948–956.
- [16] J. Baumann, D.D. Torkzadeh, A. Ramstein, U. Kiencke, T. Schlegl, Model-based predictive anti-jerk control, *Control Eng. Pract.* 14 (3) (2006) 259–266.
- [17] M. Berriri, P. Chevrel, D. Lefebvre, Active damping of automotive powertrain oscillations by a partial torque compensator, *Control Eng. Pract.* 16 (7) (2008) 874–883.
- [18] S. Zhou, P. Walker, J. Wu, N. Zhang, Power on gear shift control strategy design for a parallel hydraulic hybrid vehicle, *Mech. Syst. Sig. Process.* 159 (2021), 107798.
- [19] M. Mattsson, R. Mehler, M. Jonasson, A. Thomasson, Optimal model predictive acceleration controller for a combustion engine and friction brake actuated vehicle, *IFAC-PapersOnLine* 49 (11) (2016) 511–518, <https://doi.org/10.1016/j.ifacol.2016.08.075>.
- [20] R.S. Vadamarlu, C. Beidl, Adaptive internal model-based harmonic control for active torsional vibration reduction, *IEEE Trans. Ind. Electron.* 67 (4) (2020) 3024–3032, <https://doi.org/10.1109/TIE.2019.2908579>.
- [21] H. Yonezawa, I. Kajiwara, C. Nishidome, T. Hatano, M. Sakata, S. Hiramatsu, Active vibration control of automobile drivetrain with backlash considering time-varying long control period, *Proc. Inst. Mech. Eng. Part D J. Automob. Eng.* 235 (2-3) (2021) 773–783, <https://doi.org/10.1177/0954407020949428>.
- [22] G. Wu, X. Zhang, L. Zhu, Z. Lin, J. Liu, Fuzzy sliding mode variable structure control of a high-speed parallel PnP robot, *Mech. Mach. Theory* 162 (2021), 104349, <https://doi.org/10.1016/j.mechmachtheory.2021.104349>.
- [23] F.L. Silva, L.C.A. Silva, J.J. Eckert, M.A.M. Lourenço, Robust fuzzy stability control optimization by multi-objective for modular vehicle, *Mech. Mach. Theory* 167 (2022), 104554, <https://doi.org/10.1016/j.mechmachtheory.2021.104554>.
- [24] Y. Wang, J. Wu, N. Zhang, W. Mo, Dynamics modeling and shift control of a novel spring-based synchronizer for electric vehicles, *Mech. Mach. Theory* 168 (2022), 104586, <https://doi.org/10.1016/j.mechmachtheory.2021.104586>.
- [25] R. He, X. Tian, Y. Ni, Y. Xu, Mode transition coordination control for parallel hybrid electric vehicle based on switched system, *Adv. Mech. Eng.* 9 (8) (2017) 1–12.
- [26] Z. Song, J. Li, Z. Shuai, L. Xu, M. Ouyang, Fuzzy logic torque control system in four-wheel-drive electric vehicles for active damping vibration control, *Int. J. Veh. Des.* 68 (1/2/3) (2015), <https://doi.org/10.1504/IJVD.2015.071068>.
- [27] D. Hao, C. Zhao, Y. Huang, P. Dai, Y. Liu, Double-target switching control of vehicle longitudinal low-frequency vibration based on fuzzy logic, *Shock Vibrat.* (2018), <https://doi.org/10.1155/2018/8252815>.
- [28] J.J. Eckert, S.F. da Silva, F.M. Santicoli, A.C. Carvalho, F.G. Dedini, Multi-speed gearbox design and shifting control optimization to minimize fuel consumption, exhaust emissions and drivetrain mechanical losses, *Mech. Mach. Theory* 169 (2022), 104644, <https://doi.org/10.1016/j.mechmachtheory.2021.104644>.
- [29] H. Yonezawa, I. Kajiwara, S. Sato, C. Nishidome, M. Sakata, T. Hatano, S. Hiramatsu, Vibration control of automotive drive system with nonlinear gear backlash, *Transactions of the ASME, J. Dyn. Syst. Meas. Control* 141 (12) (2019), 121002.
- [30] H. Yonezawa, I. Kajiwara, C. Nishidome, S. Hiramatsu, M. Sakata, T. Hatano, Vibration control of automotive drive system with backlash considering control period constraint, *J. Adv. Mech. Des. Syst. Manufactur.* 13 (1) (2019) 18–00430.
- [31] H. Yonezawa, I. Kajiwara, S. Sato, C. Nishidome, T. Hatano, S. Hiramatsu, Application of physical function model to state estimations of nonlinear mechanical systems, *IEEE Access* 9 (2021) 12002–12018.
- [32] J.C. Gerdes, V. Kumar, An impact model of mechanical backlash for control system analysis, in: Proceedings of the American Control Conference ACC'95, 1995, pp. 3311–3315.
- [33] M. Nordin, J. Galic, P.-O. Gutman, New models for backlash and gear play, *Int. J. Adapt. Control Signal Process.* 11 (1997) 49–63.
- [34] B. Bamieh, J.B. Pearson, The H<sub>2</sub> problem for sampled-data systems, *Syst. Control Lett.* 19 (1992) 1–12.
- [35] P.P. Khargonekar, N. Sivashankar, H<sub>2</sub> optimal control for sampled-data systems, *Syst. Control Lett.* 17 (1991) 425–436.
- [36] T.C. Chen, B.A. Francis, H<sub>2</sub>-optimal sampled-data control, *IEEE Trans. Autom. Control* 36 (4) (1991) 387–397.
- [37] Suharjito, Dianan, Yulianto, A. Nugroho, Mobile expert system using fuzzy tsukamoto for diagnosing cattle disease, *Proc. Comput. Sci.* 116 (2017) 27–36, <https://doi.org/10.1016/j.procs.2017.10.005>.
- [38] J.-S.R. Jang, C-T. Sun, Neuro-fuzzy modeling and control, *Proc. IEEE* 83 (3) (1995) 378–406. DOI: 10.1109/5.364486.
- [39] P.K. Gupta, P.K. Muhuri, Extended Tsukamoto's inference method for solving multi-objective linguistic optimization problems, *Fuzzy Sets Syst.* 377 (2019) 102–124, <https://doi.org/10.1016/j.fss.2019.02.022>.